

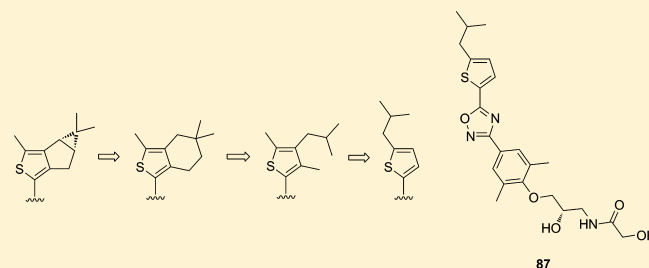
Novel S1P₁ Receptor Agonists - Part 2: From Bicyclo[3.1.0]hexane-Fused Thiophenes to Isobutyl Substituted Thiophenes

Martin H. Bolli,* Jörg Velker, Claus Müller, Boris Mathys, Magdalena Birker, Roberto Bravo, Daniel Bur, Ruben de Kanter, Patrick Hess, Christopher Kohl, David Lehmann, Solange Meyer, Oliver Nayler, Markus Rey, Michael Scherz, and Beat Steiner

Drug Discovery Chemistry, Actelion Pharmaceuticals Ltd., Gewerbestrasse 16, CH-4123 Allschwil, Switzerland

S Supporting Information

ABSTRACT: Previously, we reported on the discovery of a novel series of bicyclo[3.1.0]hexane fused thiophene derivatives that serve as potent and selective S1P₁ receptor agonists. Here, we discuss our efforts to simplify the bicyclohexane fused thiophene head. In a first step the bicyclohexane moiety could be replaced by a simpler, less rigid cyclohexane ring without compromising the S1P receptor affinity profile of these novel compounds. In a second step, the thiophene head was simplified even further by replacing the cyclohexane ring with an isobutyl group attached either to position 4 or position 5 of the thiophene. These structurally much simpler headgroups again furnished potent and selective S1P₁ agonists (e.g., **87**), which efficiently and dose dependently reduced the number of circulating lymphocytes upon oral administration to male Wistar rats. For several compounds discussed in this report lymphatic transport is an important route of absorption that may offer opportunities for a tissue targeted approach with minimal plasma exposure.



INTRODUCTION

Sphingosine 1-phosphate (S1P, Figure 1) exerts a wealth of cellular effects such as cell survival, proliferation, or migration

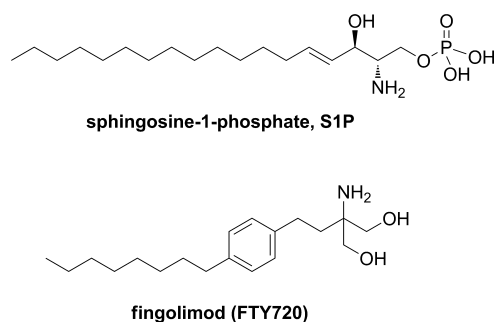


Figure 1. Structures of sphingosine 1-phosphate and fingolimod (FTY720).

by acting intracellularly as well as extracellularly.^{1–8} The extracellular signaling of S1P through five S1P receptors, numbered S1P₁ through S1P₅,⁹ has been characterized in great detail, and the large body of data has been summarized in several review articles.^{7,10–13} The pharmacological consequences of the different S1P–S1P receptor signaling cascades have been studied in many organs and tissues such as the nervous system,^{14,15} the lung,^{16,17} the cardiovascular system,^{18–26} the cells of the immune system,^{11,27,28} and bone tissue,²⁹ and as a consequence, S1P receptor modulators have been proposed to

be useful in a large number of pathological situations including autoimmune diseases, graft versus host disease, asthma, cardiovascular diseases, and cancer.^{30–32}

Of particular interest is that lymphocytes exposed to a (synthetic) S1P₁ receptor agonist are sequestered to lymphoid organs and removed from circulation. This has first been described for fingolimod (Figure 1), which is phosphorylated in vivo to become a potent nonselective S1P_{1–5} receptor agonist.^{33–40} The S1P concentration gradient⁴¹ that exists between blood plasma and lymph is seen as the driving force for T-lymphocytes to exit the lymph nodes and re-enter systemic circulation.^{11,42,43} Activation of the S1P₁ receptor is thought to lead to receptor internalization and thus desensitization of the cell toward the external S1P gradient. The desensitized lymphocytes can no longer leave the lymph node, and according to this model, the S1P₁ agonist acts as a “functional antagonist”. Indeed, recent studies demonstrated that S1P₁ antagonists are able to sequester lymphocytes from circulation.^{44,45} By use of S1P₁ receptor knockout mice^{46,47} and S1P₁ selective agonists,^{48–50} it has been demonstrated that targeting S1P₁ is sufficient to cause lymphocyte sequestration to lymphoid organs. On the other hand, activation of the S1P₃ pathway has been reported to cause heart rate reduction^{51–53} and vaso- and bronchoconstriction in rodents.^{17,54,55} It is noteworthy, however, that in the rat selectivity against the S1P₃ receptor is not sufficient for a compound to be devoid of effects

Received: September 20, 2013

Published: December 17, 2013

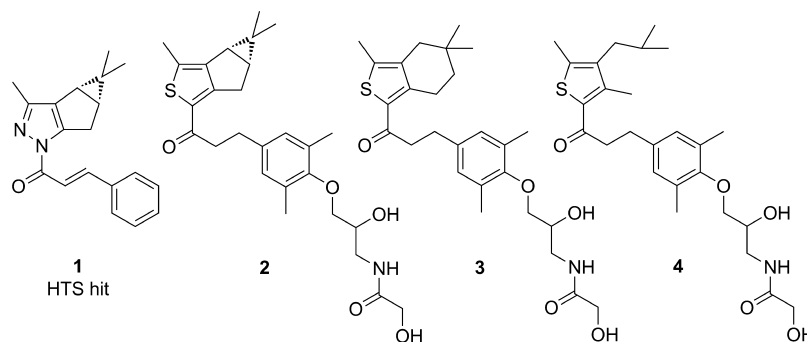


Figure 2. Structures of the original HTS hit 1 and compounds 2, 3, and 4 as examples of novel lead series derived thereof.

on heart rate and that the experimental design (e.g., single dose vs multiple dose regimen, conscious vs anesthetized animals) impacts the study outcome.^{56,57} In fact, the recent study by Fryer et al.⁵⁷ suggests that in the rat, the observed heart rate reduction is caused by S1P₁ receptor agonism while the arterial blood pressure increase is triggered by S1P₃ activation. In addition, there is growing evidence that the transient heart rate reduction observed in humans is triggered by S1P₁ receptor activation.^{58–61}

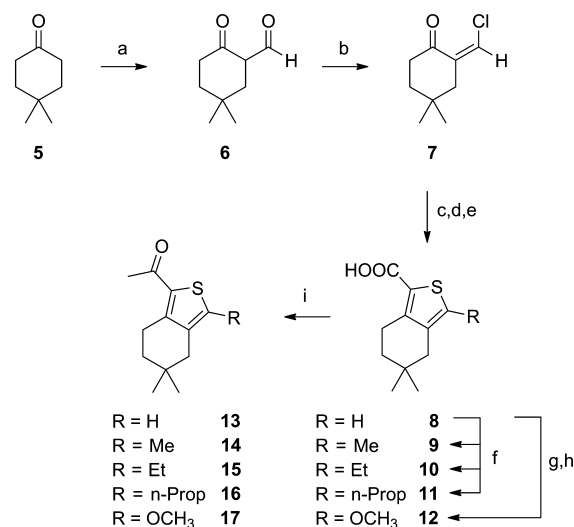
Today fingolimod is approved to treat patients suffering from multiple sclerosis (MS),^{62–64} and several S1P₁ agonists such as ponesimod,^{65–68} siponimod (BAF312),^{69–71} ONO-4641 (structure undisclosed),⁷² CS-0777,^{73,74} KRP-203,^{75–77} RPC-1063 (structure undisclosed),⁷⁸ and MT-1303 (structure undisclosed)⁷⁹ entered clinical trials for MS and other diseases. In addition, an overwhelming number of patents claiming novel selective S1P₁ receptor agonists have been published in the past few years.^{80–83}

In our previous account⁸⁴ we described the discovery of a novel series of selective S1P₁ receptor agonists. Efforts aimed at replacing the chemically unstable acylpyrazole moiety present in the original HTS hit structure 1 (Figure 2) led to the discovery of a series of bicyclo[3.1.0]hexane fused thiophene derivatives (e.g., 2, Figure 2) with high affinity and selectivity for the S1P₁ receptor. In addition, several representatives of this class of 3-carene derivatives not only exhibited good PK properties but also efficiently reduced the number of circulating lymphocytes in the rat. In this report we discuss our attempts to simplify the structure of these S1P₁ receptor agonists without compromising their favorable pharmacological profile. First, we considered opening of the 3-carene derived bicyclo[3.1.0]hexane moiety in 2 to a cyclohexane ring to give analogue 3 (Figure 2). Indeed, the cyclohexane fused thiophene 3 was as potent on the S1P₁ receptor (EC_{50} = 0.5 nM) as the bicyclo[3.1.0]hexane derivative 2 (EC_{50} 1.2 nM). In a second step, the cyclohexane ring was opened to give the 4-isopropylthiophene 4. This further simplified compound showed an EC_{50} value of 2.7 nM for S1P₁. On the basis of these observations, we decided to explore the scope of the cyclohexane fused and the isobutyl substituted thiophene derivatives in detail.

RESULTS AND DISCUSSION

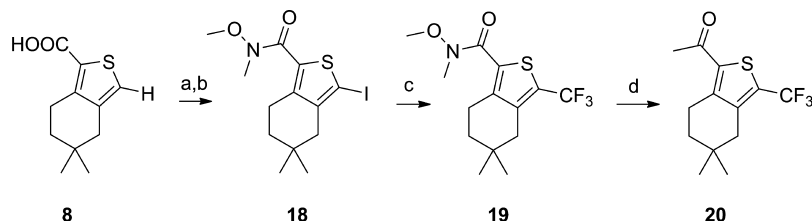
Synthesis. The synthesis of the 4,5,6,7-tetrahydrobenzo-thiophene-1-carboxylic acid scaffold is analogous to the one of the bicyclo[3.1.0]hexane fused thiophene we discussed in our previous report⁸⁴ (Scheme 1). Thus, 4,4-dimethylcyclohexanone 5 is formylated with ethyl formate in THF in the presence of potassium *tert*-butylate to give aldehyde 6 (or a

Scheme 1. Preparation of the Cyclohexane Fused Thiophen-2-ylcarboxylic Acids 8–12 and Methyl Ketones 13–17⁸⁴



^aReagents and conditions: (a) ethyl formate, KO^tBu, THF, rt, 1–24 h, 73–89% (distillation); (b) oxalyl chloride, DCM or CHCl₃, 0–30 °C, 1–18 h, 81–89% crude; (c) NaOEt, HSCH₂COOEt, EtOH, THF, rt, 1 h; (d) NaOEt, EtOH, 50–75 °C, 1–18 h; (e) 2 N aqueous LiOH or NaOH, H₂O, 70 °C, 2–3 h, 57–64% (over four steps); (f) *tert*- or *sec*-BuLi, THF, iodoalkane, –78 to –70 °C, 2–18 h, 53–86%; (g) NIS, CH₃Cl/HOAc 1:1, rt, 24 h, 58%; or 8 as ethyl ester, Br₂, AcOH, 50 °C, 4 h, 81%; (h) Cu(I) triflate, Cs₂CO₃, MeOH, 95 °C, 24 h (sealed vessel), 16–58%; (i) MeLi, diethyl ether, 20–30 °C, 1–2 h, 17–80%.

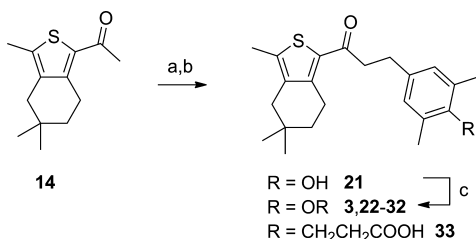
tautomer) in good yield. Chlorination to the vinyl chloride 7 was effected by treating 6 with oxalyl chloride in chloroform. The chloride 7 was then reacted using ethyl 2-mercaptoacetate,⁸⁵ and subsequent cyclization and ester hydrolysis produced the thiophenecarboxylic acid derivative 8 in good yield. It is important to note that we occasionally observed rapid, spontaneous decomposition of concentrated crude 7 when it was allowed to stand at room temperature. We therefore did not purify crude 7 any further but immediately subjected it to the substitution–cyclization sequence using ethyl mercaptoacetate. Deprotonating 8 using an excess (2.3–2.7 equiv) of *tert*- or *sec*-butyllithium at –70 to –78 °C gave the corresponding dianion which was then reacted with the appropriate iodoalkane to yield the 5-alkylated thiophenecarboxylic acids 9–11. On the other hand, exposing 8 to *N*-iodosuccinimide led to the corresponding 5-iodothiophene-2-carboxylic acid derivative which could be transformed to the 5-methoxythiophene 12 in an Ullmann-type reaction.⁸⁶ Treating the carboxylic acids 8–12 with methyl lithium furnished the

Scheme 2. Preparation of 5-Trifluoromethylthiophen-2-yl Methyl Ketone Derivative 20^a

^aReagents and conditions: (a) *N,O*-dimethylhydroxylamine HCl, TBTU, Hünig's base, DMSO, DMF, rt, 2 h, 95%; (b) LDA, I₂, THF, -78 °C, 30 min, 52%; (c) ClF₂COOMe, CuI, KF, DMF, 135 °C, 4 h, 92%; (d) MeLi, diethyl ether, 20–30 °C, 1–2 h, 75%.

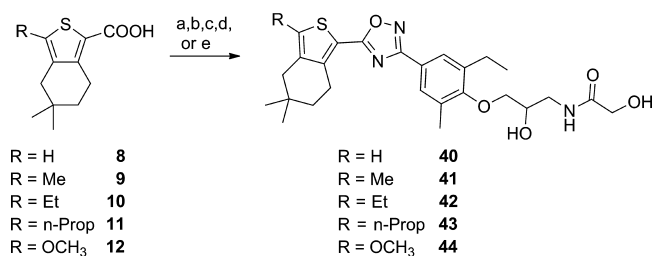
corresponding methyl ketones 13–17. The 5-trifluoromethylthiophene derivative 20 was prepared by first transforming the carboxylic acid 8 to the corresponding Weinreb amide⁸⁷ (Scheme 2). Subsequent electrophilic substitution of the thiophene carbanion with iodine gave 5-iodothiophene 18 which was reacted with methyl chlorodifluoroacetate⁸⁸ to furnish 5-trifluoromethylthiophene 19 in good yield. Finally, transforming the Weinreb amide to the corresponding methyl ketone using methyl lithium established compound 20.

The preparation of target compounds 21–33 is shown in Scheme 3. First, the methyl ketone 14 was reacted with 4-

Scheme 3^a

^aReagents and conditions: (a) 4-hydroxy-3,5-dimethylbenzaldehyde, 1 N HCl in 2-propanol, EtOH, rt, 1–2 h, 65–87%; (b) 1 bar H₂, Pd/C, EtOH, rt, 1–5 h, 78–96% (21); or 3-(4-formyl-2,6-dimethylphenyl)propenoic acid, NaOH, MeOH, rt, 3–18 h, 60–75%; (b) 10 bar H₂, Pd/C, EtOH, Hünig's base, 50–65 °C, 2–4 d; 45–78% (33); (c) 2-bromoethanol, 3-bromopropanol or (*R*)- or (*S*)-3-chloropropane-1,2-diol, 2 N aqueous NaOH, 2-propanol, 70 °C, 4–8 h, 57–74% (22–25); or 22 or 23, methanesulfonyl chloride, Hünig's base, DCM, rt, 1 h, quantitative crude, then appropriate amine, Hünig's base, DMF, 75 °C, 7 h, 58–67% (26, 27, 28); or epichlorohydrin, 3 N aqueous NaOH, 2-propanol, rt, 16–21 h, 57–91%, then 7 N NH₃ in MeOH, 65 °C, 18 h (63–91%, 29), then glycolic acid, Hünig's base, TBTU, DCM, rt, 1–2 h, 45–67% (3); or epichlorohydrin as for 3, then 2-aminoethanol, β-alanine or azetidine-3-carboxylic acid, EtOH, H₂O, Hünig's base, 85 °C, 5 h, 58–67% (30, 31, 32).

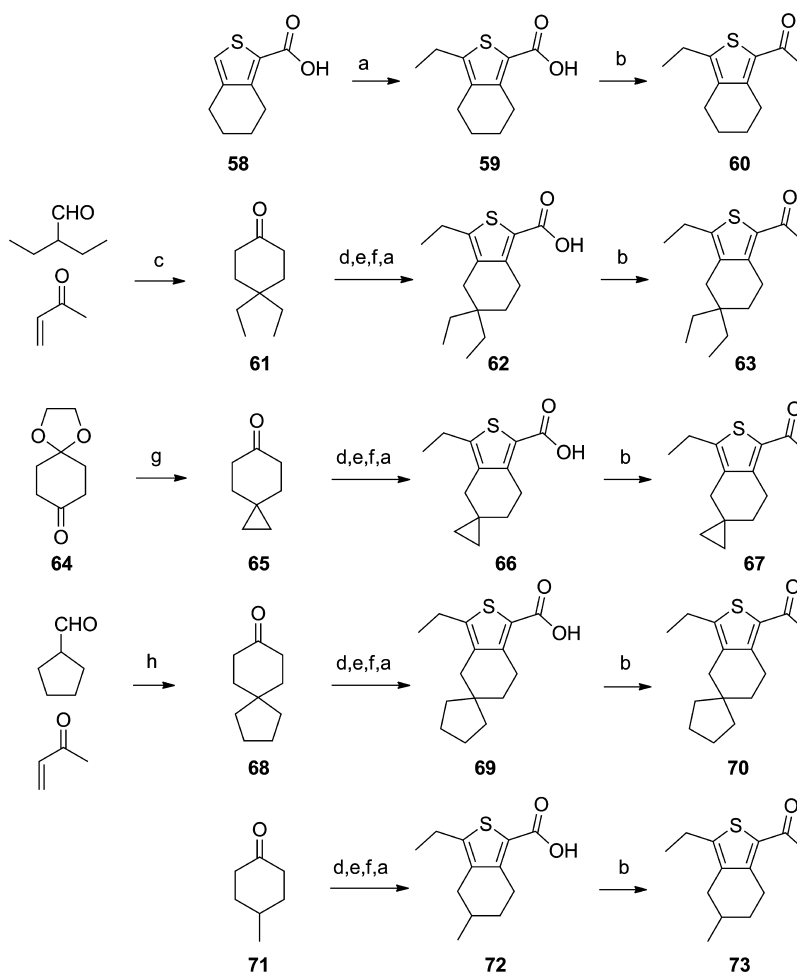
hydroxy-3,5-dimethylbenzaldehyde or 3-(4-formyl-2,6-dimethylphenyl)propenoic acid,⁸⁹ and the corresponding condensation product was hydrogenated to give phenol 21 or carboxylic acid 33, respectively. Further elaboration of side chains attached to phenol 21 as summarized in step c furnished the target compounds 22–32. Starting from the appropriate thiophene derivatives 13–17, the preparation of the corresponding glycolamide derivatives 34–39 was carried out in analogy to the pathway outlined in Scheme 3. The corresponding oxadiazole analogues 40–44 were prepared as shown in Scheme 4. Thus, coupling of the thiophenecarboxylic acids 8–11 with 3-ethyl-4,*N*-dihydroxy-5-methylbenzamidine followed by thermal dehydration to form the oxadiazole ring

Scheme 4. Preparation of Target Compounds Incorporating a [1,2,4]Oxadiazole Linker^a

^aReagents and conditions: (a) 3-ethyl-4,*N*-dihydroxy-5-methylbenzamidine, TBTU, DMF, rt, 18 h, then dioxane, 100 °C, 20 h, 59–71%; (b) (*R*)- or *rac*-epichlorohydrin, isopropanol, 3 N aqueous NaOH, rt, 20 h, 53–84%; (c) 7 N NH₃ in methanol, 65 °C, 18 h, 86% quantitative (crude); (d) glycolic acid, TBTU, Hünig's base, DCM, rt, 2–4 h, 36–70%; (e) (for 44) (*S*)-*N*-(3-(2-ethyl-4-(*N*-hydroxycarbonylmimido)-6-methylphenoxy)-2-hydroxypropyl)-2-hydroxyacetamide, EDC, HOBT, DMF, rt, 24 h, then dioxane, 100 °C, 24 h, 6%.

(step a) and subsequent elaboration of the polar side chain (steps b–d) produced the compounds 40–43. Alternatively, as illustrated with the methoxythiophene derivative 44, the thiophene-2-carboxylic acid can also be coupled and cyclized with an *N*-hydroxybenzamidine building block already incorporating the glycolamide side chain.

The thiophenecarboxylic acids 59, 62, 66, 69, and 72 and the thienyl methyl ketones 60, 63, 67, 70, and 73 required to prepare target compounds 54–57 and 45–50 (Table 3), respectively, were obtained following the pathway outlined in Scheme 5. The precursor of 59, 4,5,6,7-tetrahydrobenzo[*c*]thiophene-1-carboxylic acid 58 (for target compounds 45 and 54), is commercially available. Preparation of 62 (for 47 and 55) relied on 4,4-diethylcyclohexanone 61.^{90,91} Spiro[2.5]octan-6-one 65 needed for the preparation of 66 (for 48 and 56) was prepared starting from acetal 64 following literature procedures.^{92–94} The starting material for thiophenecarboxylic acid 69 (for 49 and 57), spiro[4.5]decan-8-one 68, was also prepared following literature procedures.^{91,95} 4-Methylcyclohexanone 71 needed for the synthesis of thiophene 72 (for 50) is commercially available. The carboxylic acids 59, 62, 66, 69, and 72 were then transformed to the corresponding ketones 60, 63, 67, 70, and 73, respectively, by treating them with methyl lithium. Scheme 6 outlines the synthetic access to 5-hydroxytetrahydrobenzo[*c*]thiophenes 77 and 78 which served as starting materials for the preparation of 51 and 52, respectively. In brief, thiophene-2-carboxylic acid 74 was obtained from cyclohexanone 64 following our standard formylation–chlorination–substitution–cyclization–alkylation sequence. Weinreb amide⁸⁷ formation followed by acetal

Scheme 5. Preparation of 5-Mono- or Disubstituted 3-Ethyl-4,5,6,7-tetrahydrobenzo[*c*]thiophene-1-carboxylic Acids and 1-(3-Ethyl-4,5,6,7-tetrahydrobenzo[*c*]thiophen-1-yl)ethanones^a

^aReagents and conditions: (a) ^tBuLi, THF, EtI, -100 to -70 °C, 2–18 h, 31–85%; (b) MeLi, diethyl ether, 20–30 °C, 1–2 h, 33–66%; (c) H₂SO₄, rt, 24 h, 70%, then 1 bar of H₂, Pd/C, EA, rt, 24 h, quantitative;^{90,91} (d) ethyl formate, KO^tBu, THF, rt, 24 h; (e) oxalyl chloride, DCM or CHCl₃, 0–30 °C, 1–18 h; (f) (1) NaOEt, HSCH₂COOEt, EtOH, rt, 1 h; (2) NaOEt, EtOH, 65–75 °C, 18 h; (3) 2 N aqueous LiOH or NaOH, H₂O, 70 °C, 2–3 h; 23–47% (over steps d, e, f, b); (g) (1) Ph₃PMeBr, NaH, toluene, DMSO, rt, 1 h, quantitative (crude);^{92,94} (2) Et₂Zn, CH₂I₂, toluene, -40 °C to rt, 18 h, then TFA, H₂O, rt, 30 min, 90% (crude);^{93,94} (h) (1) piperidine, ethanol, 85 °C, 24 h, then NaOAc, HOAc, 85 °C, 24 h, 63%; (2) 1 atm of H₂, Pd/C, EA, rt, 90 min, 97%.^{91,95}

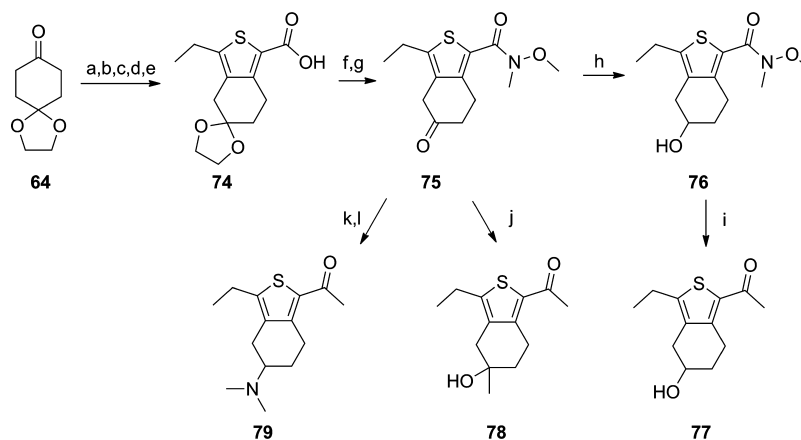
cleavage delivered ketone **75** which was then reduced to the corresponding alcohol **76**. Exposing Weinreb amides **76** and **75** to the methyl Grignard reagent produced methyl ketones **77** and **78**, respectively. On the other hand, reductive amination of ketone **75** with dimethylamine followed by Grignard reaction furnished the racemic ketone **79** in good yield (steps k and l). Starting from the appropriate thiophenyl methyl ketones and thiophene-2-carboxylic acids shown in Schemes 5 and 6, compounds **45–57** (Table 3) were prepared in analogy to the reactions outlined in Schemes 3 and 4.

Synthesis of alkylated thiophene-2-carboxylic acids **94**, **96**, **97**, and **99–102**, which were used to prepare the target compounds **81–90** (Table 5), is shown in Scheme 7. Formylation of isopentyl methyl ketone **91** using ethyl formate under basic conditions furnished enol **92** (or tautomer) which was treated with oxalyl chloride at room temperature to give vinyl chloride **93**. Reacting **93** with ethyl mercaptoacetate in the presence of a base furnished 4-isobutyl-3-methylthiophene-2-carboxylic acid **94**. Conversely, if ketone **91** was formylated under Vilsmeier conditions, the isomeric vinyl chloride **95** was

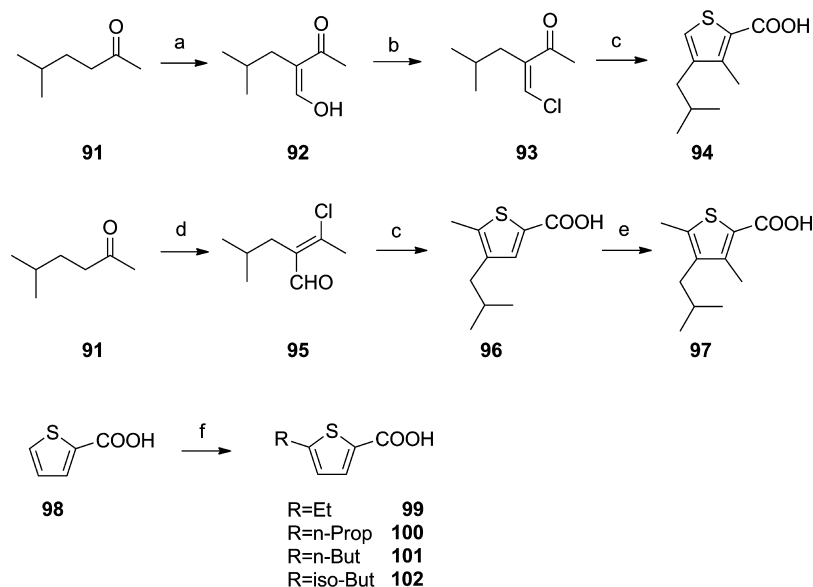
obtained. Treating this material with ethyl mercaptoacetate delivered 4-isobutyl-5-methylthiophene-2-carboxylic acid **96** which could be further alkylated using *tert*-butyllithium followed by methyl iodide to give the 3,5-dimethyl substituted thiophene derivative **97**. Finally, alkylation of thiophene-2-carboxylic acid **98** using LDA or *tert*-butyllithium and an alkyl halide to give the 5-alkylated thiophene-2-carboxylic acids **99–102** was performed following literature procedures.⁹⁶ The target compounds **81–90** were then prepared in analogy to the pathway shown in Scheme 4.

The target compounds **4** and **80** were prepared starting from thiophenecarboxylic acids **97** and **102**, respectively, in analogy to the pathways outlined in Schemes 5 and 3.

In Vitro SAR Discussion. For the following discussion, the compounds' potencies were assessed using a GTPγS assay with membranes from CHO cells expressing either the recombinant S1P₁ or S1P₃ receptor. Table 1 compiles a first set of compounds wherein the polar side chain attached to the phenyl ring has been varied. As already observed in the 3-carene derived series,⁸⁴ a large variety of polar side chains was

Scheme 6^a

^aReagents and conditions: (a) ethyl formate, KO^tBu, THF, rt, 24 h, 60–65%; (b) oxalyl chloride, CHCl₃, rt, 30 min, 88% crude; (c) NaOEt, HSCH₂COOEt, EtOH, 30 °C, 2 h, 46%; (d) 1 N aqueous NaOH, EtOH, 70 °C, 1 h, 98%; (e) ^tBuLi, EtI, THF, –100 to –80 °C, 8 h, 50%; (f) *N,O*-dimethylhydroxylamine HCl, TBTU, Hünig's base, DMF, rt, 3 h, 92%; (g) 2 N aqueous HCl, THF, 40 °C, 2 h, 96%; (h) NaBH₄, MeOH, rt, 1 h, quantitative crude; (i) MeMgBr, THF, rt, 18 h, 82%; (j) MeMgBr, THF, rt, 3 h, 40–45%; (k) HNMe₂, NaBH(OAc)₃, EtOH, rt, 18 h, 50–66%; (l) MeMgBr, THF, rt, 3 h, 80% to quantitative (crude).

Scheme 7. Preparation of Thiophene-2-carboxylic Acids^a

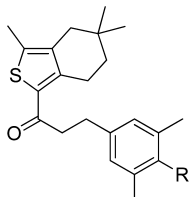
^aReagents and conditions: (a) ethyl formate, KO^tBu, THF, 0 °C to rt, 15 h, 66%; (b) oxalyl chloride, CHCl₃, rt, 2 h, quantitative crude; (c) (1) NaOEt, HSCH₂COOEt, EtOH, rt, 15 h; (2) NaOEt, EtOH, 85 °C, 1 h; (3) 2 N aqueous LiOH, EtOH, rt, 48 h, 28–41%; (d) POCl₃, DMF, 0 °C, 30 min, rt, 3 h, quantitative crude; (e) ^tBuLi, THF, MeI, –78 °C, 2 h, 65%; (f) LDA or ^tBuLi, THF, alkyl iodide or bromide, –78 °C, 2 h, 15–68%.

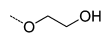
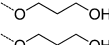
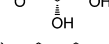
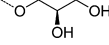
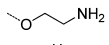
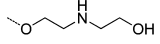
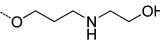
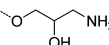
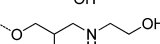
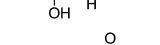
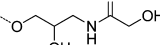
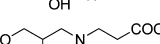
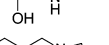
tolerated at the phenyl ring and the relative potency order was preserved between the two series. In general, the cyclohexane fused thiophene derivatives were slightly less potent on both S1P₁ and S1P₃.

Thus, while both glycerol derivatives **24** and **25** reached single digit nanomolar activity with several-hundred-fold selectivity against S1P₃, the phenol **21** and the ethylene and propylene glycol derivatives **22** and **23** showed a slightly reduced affinity for S1P₁. The amine **26** was more potent on S1P₁ when compared to its alcohol analogue **22**. The opposite trend was observed when the (racemic) amine **29** was compared to the corresponding glycerol analogues **24** and **25**. Adding a hydroxyethyl chain to amines **26** and **29** (compounds **27**, **28**, **30**) reduced the compound's affinity for S1P₁. On the other hand, masking the basic nitrogen in

compound **30** by forming glycolamide **3** improved the compound's affinity for S1P₁ and S1P₃ significantly. Interestingly, compounds **31** and **32** combining a basic nitrogen with a carboxylic acid in their side chain again showed high affinity for the S1P₁ receptor and maintained good selectivity against S1P₃. The much shorter propanoic acid side chain in **33** led to a reduced potency on both receptors.

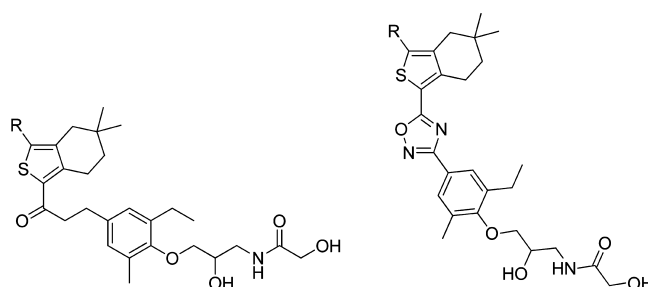
In contrast to the carene derivatives, the 4,5,6,7-tetrahydrobenzo[*c*]thiophene series allowed for easy synthetic access to a variety of scaffolds with different 3-substituents (benzo[*c*]thiophene numbering). Therefore, the influence of the 3-substituent could be studied in more detail. The SAR is illustrated with a set of compounds incorporating a "glycolamide" side chain and includes propanone (**34–39**) or oxadiazole (**40–44**) linked derivatives (Table 2). In general,

Table 1. SAR of Polar Side Chains in the 4-Position of the Phenyl Ring^a


Compound	R	EC ₅₀ S1P ₁ [nM]	EC ₅₀ S1P ₃ [nM]
2	- ^b	1.2	430
21	OH	21	>10000
22		19	4447
23		71	4450
24		2.6	1400
25		3.4	1098
26		6.1	8558
27		11	>10000
28		48	>10000
29		7.0	>10000
30		14	>10000
3		0.5	392
31		1.2	569
32		4.3	1755
33		21	>10000

^aEC₅₀ values as determined in a GTPγS assay using membranes of CHO cells expressing either S1P₁ or S1P₃. EC₅₀ values represent geometric mean values of at least three independent measurements in duplicate. All compounds with EC₅₀ ≤ 1 μM behaved as full agonists on S1P₁ and S1P₃ (E_{max} > 85%). For compounds with EC₅₀ > 1 μM it was not possible to determine whether or not they are full agonists because no activity plateau was reached at the highest compound concentration tested (10 μM). For details see Experimental Section. ^bFor comparison, for structure see Figure 2.

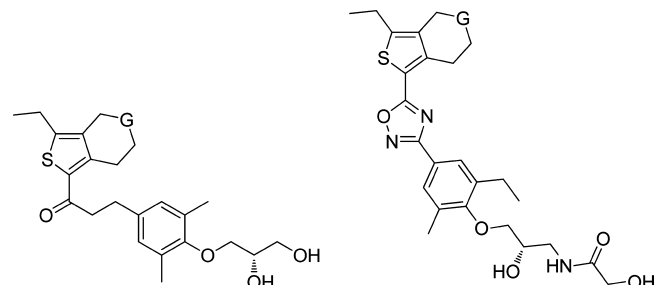
both linkers led to potent S1P₁ agonists. The propanone linked compounds were consistently more selective against S1P₃. In both linker series, the 3-unsubstituted compounds (34 and 40) showed high affinity and more than 100-fold selectivity for the S1P₁ receptor. In the propanone linked series, increasing the size of the 3-substituent from hydrogen to an *n*-propyl group had little effect on the S1P₁ receptor affinity while the potency on S1P₃ increased steadily. The affinity profile of the trifluoromethyl derivative 38 resembled the one of the ethyl analogue 36, while the methoxythiophene 39 showed almost identical potencies as the methyl analogue 35. The oxadiazole derivatives, too, gained potency on S1P₃ with increasing chain length of the 3-substituent. But they lost potency on S1P₁ in going from 40 to 43 making the *n*-propyl derivative 43 the least selective compound of this set. As before, the affinity profile of the methoxythiophene 44 was very similar to the one of the methyl analogue 41.

Table 2. SAR of the 3-Substituent at the 4,5,6,7-Tetrahydrobenzo[*c*]thiophene^a

R	propanone	EC ₅₀ S1P ₁ [nM]	EC ₅₀ S1P ₃ [nM]	oxadiazole	EC ₅₀ S1P ₁ [nM]	EC ₅₀ S1P ₃ [nM]
H	34	4.8	5270	40	1.7	314
methyl	35	1.2	4418	41	1.5	122
ethyl	36	0.6	141	42 ^c	4.6	8.9
<i>n</i> -propyl	37	1.3	25	43	20	11
CF ₃	38	1.3	242	<i>b</i>		
OCH ₃	39	1.3	3910	44	1.8	83

^aEC₅₀ values as determined in a GTPγS assay using membranes of CHO cells expressing either S1P₁ or S1P₃. EC₅₀ values represent geometric mean values of at least three independent measurements in duplicate. All compounds with EC₅₀ ≤ 1 μM behaved as full agonists on S1P₁ and S1P₃ (E_{max} > 85%). For compounds with EC₅₀ > 1 μM it was not possible to determine whether or not they are full agonists because no activity plateau was reached at the highest compound concentration tested (10 μM). For details see Experimental Section. ^bCompound not prepared. ^cPure (*S*)-enantiomer only. Studies on earlier series and close analogues of compounds discussed in this account (cf. compounds 23 and 24) showed only little differences between the two enantiomers with respect to S1P receptor affinity.

Several 4-substituted cyclohexanones are either commercially available or easily accessible by short syntheses. Using these cyclohexanones as starting materials in our standard thiophene synthesis allowed for a rapid assembly of a collection of 4,5,6,7-tetrahydrobenzo[*c*]thiophene scaffolds with a variety of substituents in position 5. Compounds with either a propanone or an oxadiazole linker were prepared. For the following SAR discussion propanone derivatives with a glycerol side chain and oxadiazoles incorporating a glycolamide side chain have been compiled in Table 3. As already seen with the compounds in Table 2, the propanone linked derivatives were clearly more selective against S1P₃. In the propanone series, removal of the two 5-methyl groups (compound 45) led to a clear loss in affinity for S1P₁, while the same modification in the oxadiazole linked series (compound 54) slightly improved the compound's potency on S1P₁. The various 5-substituents showed little difference on the S1P₁ receptor affinity of propanones 46–50 and oxadiazoles 42 and 55–57. On the other hand, the affinity for the S1P₃ receptor increased with increasing size of the substituents in position 5. As a consequence, the two diethyl substituted compounds 47 and 55 are the least selective representatives of the propanone and the oxadiazole series, respectively. Interestingly, forming a ring between the two alkyl groups in position 5 clearly improved the selectivity against S1P₃ (compare 48 with 46, 56 with 42, 49 with 47, and 57 with 55), and the cyclopropyl derivative 48 was the most selective example of the propanone series. In the oxadiazole series, the cyclopropyl derivative 56 was clearly more selective than its dimethyl analogue 42 but did not reach the selectivity of the unsubstituted compound 54. An alcohol function (compounds

Table 3. SAR of the Substituent at the Cyclohexane Ring^a


G	propanone	EC ₅₀ S1P ₁ [nM]	EC ₅₀ S1P ₃ [nM]	oxadiazole	EC ₅₀ S1P ₁ [nM]	EC ₅₀ S1P ₃ [nM]
-CH ₂ -	45	20	3830	54	0.9	172
	46	0.4	126	42	4.6	8.9
	47	0.4	25	55	6.0	1.2
	48	1.1	819	56	1.1	24
	49	0.4	62	57	4.7	11
	50^c	1.6	599	^b		
	51^c	860	>10000	^b		
	52^c	79	>10000	^b		
	53^c	1600	>10000	^b		

^aEC₅₀ values as determined in a GTPγS assay using membranes of CHO cells expressing either S1P₁ or S1P₃. EC₅₀ values represent geometric mean values of at least three independent measurements in duplicate. All compounds with EC₅₀ ≤ 1 μM behaved as full agonists on S1P₁ and S1P₃ (E_{max} > 85%). For compounds with EC₅₀ > 1 μM it was not possible to determine whether or not they are full agonists because no activity plateau was reached at the highest compound concentration tested (10 μM). For details see Experimental Section. ^bCompound not prepared. ^cAs an approximately 1:1 mixture of epimers.

51 and **52**) or a dimethylamino group (compound **53**) in position 5 of the tetrahydrobenzo[*c*]thiophene scaffold was obviously not tolerated.

Knowing that opening of the bicyclo[3.1.0]hexane system (as in **2**) to a cyclohexane yielded highly potent and selective S1P₁ agonists, we then studied further simplifications of the cyclohexane fused thiophene moiety. We therefore prepared a series of compounds wherein the cyclohexane ring was opened (Figure 3). The compounds compiled in Table 4 and Table 5

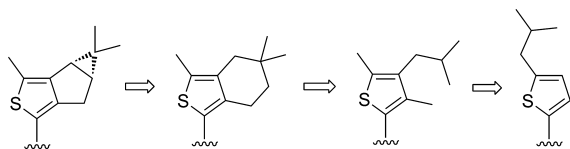
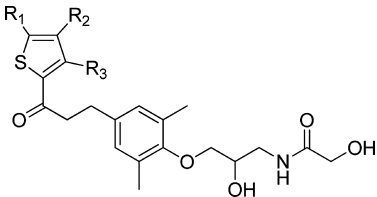


Figure 3. Simplifying the bicyclo[3.1.0]hexane fused thiophene head.

illustrate our findings. In the propanone linked series (Table 4), the carene derivative **2** and the cyclohexane fused thiophene **3** showed a nearly identical affinity profile for S1P₁ and S1P₃. Also the 4-isobutyl-3,5-dimethylthiophene **4** was almost identical in potency on S1P₁. This compound, however, was clearly more selective against S1P₃ when compared to its (bi)cyclic analogues **2** and **3**. Interestingly, moving the isobutyl

substituent to position 5 and omitting additional methyl groups at the thiophene head to give compound **80** reduced the compound's affinity for S1P₁ only slightly and increased the potency on S1P₃. In the oxadiazole linked series (Table 5), the bicyclo[3.1.0]hexane **81** and the cyclohexane **82** were highly potent on S1P₁. The exact ring-opened analogue of cyclohexane **82**, compound **83**, was slightly less active on both receptors than compound **82**. Replacing the ethyl group in R₃ by a methyl group (**84**) or a hydrogen (**86**) restored the compound's affinity for S1P₁ and reduced the potency on S1P₃. On the other hand, omitting the 5-methyl group (R₁) in **84** to give compound **85** not only enhanced the potency on S1P₁ but also significantly improved the selectivity against S1P₃, a trend already observed in the cyclohexane fused thiophene series (see Table 2). On the other hand, removing the 3-methyl group in **84** to give **86** had a less pronounced effect on the compound's affinity profile. In contrast to the observations with the two propanone derivatives **80** and **4**, the 5-isobutylthiophene **87** retained the potency on S1P₁ and lost affinity for S1P₃ when compared to the 4-isobutylthiophene **86**. While the 5-*n*-butyl and the 5-ethyl analogues **88** and **90**, respectively, were both less potent on S1P₁ and S1P₃, the 5-*n*-propyl substituted thiophene **89** is comparable to **87** on S1P₁ but more selective against S1P₃. In brief, the data on the oxadiazoles in Table 5 illustrate that while the S1P₁ receptor tolerates a large

Table 4. SAR of Substitution Pattern around the Thiophene Ring in the Propanone Series^a


Compound	R ₁	R ₂	R ₃	EC ₅₀ S1P ₁ [nM]	EC ₅₀ S1P ₃ [nM]
2 ^b	CH ₃			1.2	428
3 ^c	CH ₃			0.5	365
4 ^c	CH ₃		CH ₃	2.7	5270
80	isobutyl	H	H	7.7	590

^aEC₅₀ values as determined in a GTPγS assay using membranes of CHO cells expressing either S1P₁ or S1P₃. EC₅₀ values represent geometric mean values of at least three independent measurements in duplicate. All compounds with EC₅₀ ≤ 1 μM behaved as full agonists on S1P₁ and S1P₃ (E_{max} > 85%). For compounds with EC₅₀ > 1 μM it was not possible to determine whether or not they are full agonists because no activity plateau was reached at the highest compound concentration tested (10 μM). For details see Experimental Section. ^bCompound represents a 1:1 mixture of epimers with respect to polar side chain. ^cCompound represents racemate.

variety of alkyl substituted thiophene heads, the S1P₃ receptor is clearly more susceptible to changes in this part of the molecule. This is most impressively demonstrated by comparing the cyclohexane fused thiophene derivative **82** with the 5-propyl substituted analogue **89**. The large structural difference between these two compounds has no effect on S1P₁ affinity but evokes an 80-fold potency shift on S1P₃. The EC₅₀ values for the propanone derivatives compiled in Table 4 confirm earlier observations that in this series the affinity toward the S1P₃ receptor is consistently lower than in the oxadiazole series.

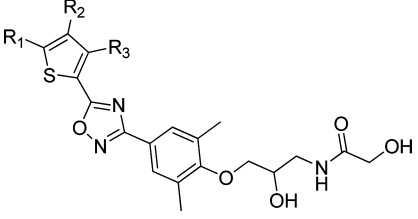
The similarity of the various thiophene headgroups becomes apparent when the X-ray crystal structures of the corresponding thiophene-2-carboxylic acids **103**, **9**, and **97** are superimposed (Figure 4). The substituents decorating the three thiophene-2-carboxylic acids assume conformations that overlap considerably suggesting overall very similar steric demands and space filling properties of these thiophene derivatives. While **103** comprises literally no degree of rotational freedom, cyclohexane **9** is more flexible because the ring pucker in **9** could switch, leading to a minor change in space filling. In **97** two preferred orientations of the isobutyl side chain (above or below the thiophene plane) are conceivable; however, the two neighboring methyl groups constrain its free rotation.

In Vivo Studies. In the course of establishing the SAR on the S1P₁ and S1P₃ receptor, we also studied the DMPK properties of selected compounds. In vitro metabolic stability data showed a clear difference between the propanone and the oxadiazole linked compounds, and we anticipated that the propanone linked derivatives would be clearly inferior with respect to pharmacokinetics (PK) and in particular pharmacodynamics (PD). We therefore selected compound **36** as the most potent representative of the propanone series and its

oxadiazole analogue **42** to illustrate the typical PK and PD behavior of the two subseries. In vitro and in vivo PK data of the two compounds are listed in Table 6. In rat liver microsomes and hepatocytes propanone **36** showed a much higher in vitro clearance than oxadiazole **42**. Similarly, a marked difference in in vivo clearance was observed between the two compounds upon iv administration of 1 mg/kg to Wistar rats. As both compounds had a comparable volume of distribution (V_{ss}), plasma concentrations of compound **36** dropped with a half-life (t_{1/2}) of 1.7 h while compound **42** showed a half-life of 21 h. The high clearance observed with propanone **36** results in low exposure (C_{max} AUC_{0–24h}) after oral dosing (Table 6).

At this point, we decided to compare the pharmacodynamic behavior of compounds **36** and **42** with their respective PK profile. Hence, the compounds were administered at a dose of 10 mg/kg to male Wistar rats and the blood lymphocyte count (LC) was measured shortly before and 3, 6, and 24 h after compound administration. A LC reduction of ≥60% was considered to be the maximal effect (plateau) to be observed under the conditions of the experiment.⁶⁵ The different pharmacokinetic properties of the two compounds clearly reflected their pharmacodynamic behavior (Figure 5). While the highly potent propanone **36** maximally reduced LC at 3 and 6 h (plasma concentrations of 32 and 10 ng/mL, respectively) and showed complete recovery of the LC at 24 h (plasma concentration of <1.5 ng/mL) after compound administration, the less potent oxadiazole **42** showed maximal LC reduction for at least 24 h (plasma concentration at 24 h of 530 ng/mL) and a still significant effect on LC after 3 and 6 days (plasma concentrations of 236 and 66 ng/mL, respectively) because of significantly higher plasma concentrations.

In two recent studies, compounds that did not produce a sustained 24 h maximal LC reduction after single dose administration have been shown to be efficacious in the mouse EAE model of multiple sclerosis, suggesting that sustained maximal LC reduction is not mandatory to obtain in vivo efficacy in this model.^{97,98} On the other hand, in clinical studies transient heart rate reduction after oral dosing of (selective) S1P₁ receptor agonists has been observed.^{58–61} Model studies in guinea pigs suggested that the S1P₁ receptor is rapidly desensitized upon activation by a S1P₁ receptor agonist and sustained plasma concentrations of the agonist protect the animal from second dose effects on heart rate.⁹⁹ A sustained 24 h plasma exposure, and as a consequence a sustained LC count reduction in the rat, therefore appeared desirable from a compound safety and efficacy perspective. Bearing this in mind, we studied the in vivo efficacy of the oxadiazole derivatives **81–90** (Table 5) at an oral dose of 10 mg/kg. All compounds showed a rapid onset of action, and with the exception of compound **83**, all compounds reached maximal LC reduction 3 h after compound administration. The duration of action, however, varied significantly between the various thiophene derivatives. While compound **81** maximally reduced LC for at least 24 h and complete recovery of LC was observed at 96 h, cyclohexane derivative **82** fully sequestered circulating lymphocytes for at least 72 h and LC recovery was seen after 168 h only. The 4-isobutyl substituted thiophenes **84**, **85**, and **86** maximally reduced LC for at least 24 h. Rapid reversibility of the LC reduction could be observed when compound **85** was administered at a lower dose of 3 mg/kg. At this dose, LC was maximally reduced at 6 h but was already close to baseline values 24 h after compound administration.

Table 5. SAR of Substitution Pattern around the Thiophene Ring in the Oxadiazole Series^a


Compound	R ₁	R ₂	R ₃	EC ₅₀ [nM]		% LC ^d		
				S1P ₁	S1P ₃	3 h	6 h	24 h
81^b	CH ₃			1.4	66	-66	-69	-73 ^e
82^c	CH ₃			1.6	15	-70	-73	-77 ^f
83^c	CH ₃		CH ₂ CH ₃	6.6	172	-30	-40	-25
84^c	CH ₃		CH ₃	0.5	74	-78	-86	-93
85^c	H		CH ₃	1.5	528	-72 -67 ^g	-79 -79 ^g	-80 -27 ^g
86^c	CH ₃		H	1.5	236	-77	-78	-91
87^c		H	H	0.6	247	-75	-79	-66 ^h
88^c		H	H	4.7	1253	-66	-52	+18
89^c		H	H	0.9	1150	-65	-59	+31
90^c		H	H	4.3	1860	-73 ⁱ	-77 ⁱ	+12 ⁱ

^aEC₅₀ values as determined in a GTPγS assay using membranes of CHO cells expressing either S1P₁ or S1P₃. EC₅₀ values represent geometric mean values of at least three independent measurements in duplicate. All compounds with EC₅₀ ≤ 1 μM behaved as full agonists on S1P₁ and S1P₃ (E_{max} > 85%). For compounds with EC₅₀ > 1 μM it was not possible to determine whether or not they are full agonists because no activity plateau was reached at the highest compound concentration tested (10 μM). For details see Experimental Section. ^bCompound represents 1:1 mixture of epimers at polar side chain. ^cRacemic compound. ^dLymphocyte counts in Wistar rats receiving 10 mg/kg compound po. ^e+30% at 96 h. ^f-73% at 72 h, -7% at 144 h. ^gAfter administration of 3 mg/kg. ^h+14% at 72 h. ⁱIn vivo data of pure (S)-enantiomer.

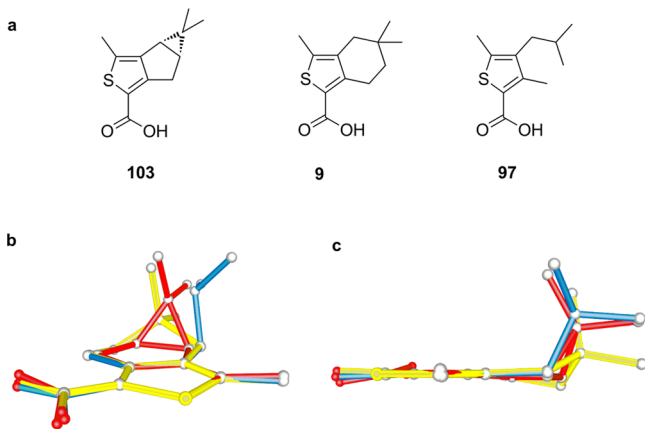


Figure 4. Structures (a) and superposition of the X-ray structures (b, c) of the three thiophene-2-carboxylic acids **103** (red), **9** (yellow), and **97** (blue) using the thiophene ring as the anchor unit.

In the series of the 5-alkylthiophenes **87–90**, only the isobutyl derivative **87** was able to maximally sequester blood lymphocytes for 24 h. The *n*-butyl (**88**), the *n*-propyl (**89**), and the ethyl (**90**) thiophenes all showed complete recovery of LC 24 h after compound administration. This observation could be rationalized on the basis of the compounds' plasma exposures. For instance, while the isopropylthiophene **87** showed plasma

Table 6. Rat PK Data of Propanone **36** and Oxadiazole **42**^a

parameter	36	42
Experiment: In Vitro		
intrinsic clearance, rat microsomes [(μL/min)/mg]	>1250	0
rat hepatocytes [(μL/min)/10 ⁶ cells]	107	3.1
Experiment: In Vivo, 1 mg/kg iv		
clearance in vivo [(mL/min)/kg]	46	2.0
V _{ss} [L/kg]	2.8	3.5
t _{1/2} in vivo [h]	1.7	21
Experiment: In Vivo, 10 mg/kg po		
AUC _{0–24h} [ng·h/mL]	276	28100
C _{max} [ng/mL]	141	1450
T _{max} [h]	0.5	6.0
bioavailability F [%]	8	>33 ^b

^aPK parameters obtained in Wistar rats after oral administration of 10 mg/kg and iv administration of 1 mg/kg of either **36** or **42**; for details see Experimental Section. ^bBioavailability cannot be determined accurately, as sampling time was up to 24 h only.

concentrations of 1010, 680, and 23 ng/mL at 3, 6, and 24 h after oral administration, respectively, the concentrations of the ethyl analogue **90** were 490, 190, and <2 ng/mL at these time points.

Lymphocytes leave lymph nodes by migrating along a gradient of S1P that exists between plasma and lymph. Synthetic S1P₁ receptor agonists lead to S1P₁ receptor

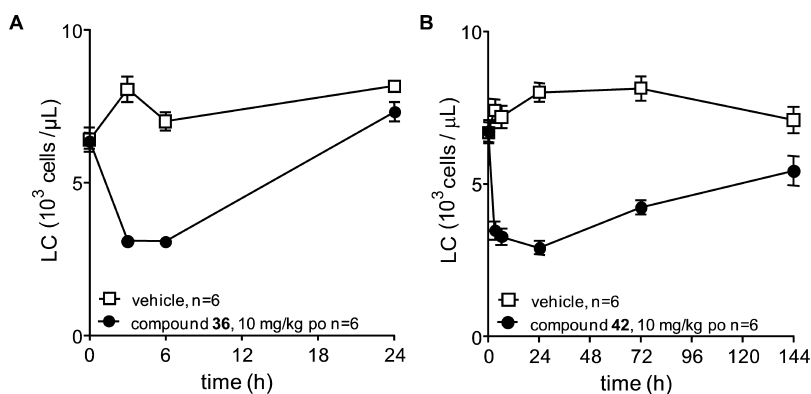


Figure 5. Lymphocyte counts measured after administration of 10 mg/kg of either ketone **36** (A) or oxadiazole **42** (B) to male Wistar rats. Note the different range of the time axis for the two graphs.

internalization and thus abolish the lymphocyte's ability to sense the S1P gradient and to leave the lymph node. The concentration of the synthetic S1P₁ agonist in lymph can be expected to influence the agonist's pharmacodynamic behavior.^{11,42,43} We thus extended the above rat PK studies and measured the concentration of compound **42** in mesenteric lymph fluid that was collected over periods of 20 min at several time points after oral administration of 10 mg/kg compound **42**. In the middle of each lymph collection period, a plasma sample was drawn as well. The compound concentrations summarized in Table 7 demonstrate that for the first few hours

Table 7. Concentration of Compound 42 in Plasma and Mesenteric Lymph after Oral Administration of 10 mg/kg to Wistar Rats

sample time ^a [h]	42 concentration [ng/mL]	
	plasma	mesenteric lymph
1.0	44.4	5790
1.7	58.1	4340
2.3	123	4600
3.0	132	8090
6.0	911	4590
24.8	680	684

^aMean of collection interval given for mesenteric lymph.

the concentration of compound **42** in mesenteric lymph fluid exceeded the one in plasma by far, indicating that there is significant lymphatic transport of the compound after oral dosing. The compound was quickly absorbed into mesenteric lymph, reaching a concentration of nearly 6000 ng/mL at 1 h after administration. Plasma concentrations increased much more slowly and reached a significantly lower C_{max} . Compound concentrations in plasma and mesenteric lymph were equal at 24 h after compound administration, suggesting equilibration of the compound between the two compartments. As a consequence of the rapid and pronounced lymphatic transport of compound **42**, the exposure (AUC_{0-t}) in mesenteric lymph was significantly higher than in plasma. Although our experimental setup does not allow calculation of the fraction of the dose that undergoes lymphatic transport, lymphatic exposure and thus lymphatic transport are significant. The high lymph exposure of compound **42** may contribute to the compound's in vivo efficacy.

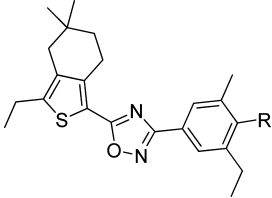
Compound concentrations in lymph fluids are not determined regularly. However, it is generally accepted that

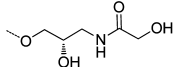
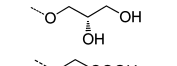
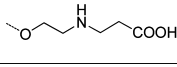
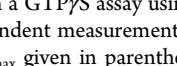
lipophilicity is a clear driver of lymphatic transport.^{100,101} The high lipophilicity ($\log D = 4.3$) of compound **42** and its lipid-like structure may thus explain its propensity for high lymphatic transport. Prompted by this interesting observation, the lymphatic route of absorption was studied for a few closely related analogues of amide **42** (Table 8, EC_{50} values on S1P₁ and S1P₃ are given for completeness). Not surprisingly, the more lipophilic diol **104** ($\log D = 5.4$) showed a very similar behavior. The compound was rapidly absorbed into mesenteric lymph, reaching a C_{max} that is remarkably higher than in plasma. Mesenteric lymph exposure was again significantly higher than plasma exposure. Despite their ionic/zwitterionic nature, the acid **105** and the amino acid **106** appear rather lipophilic ($\log D$ of 3.6 and 4.9, respectively) and showed significant lymphatic transport as well.

CONCLUSIONS

By replacing the bicyclo[3.1.0]hexane by a cyclohexane or an isobutyl group, we were able to reduce the structural complexity and rigidity of our S1P₁ agonists such as **2** without compromising their in vitro potency and in vivo efficacy. For these novel thiophene derivatives the SARs of the polar side chain and the linker between the thiophene and the phenyl ring bearing the polar side chain were similar to those previously reported for the bicyclo[3.1.0]hexane fused thiophene series.⁸⁴ The easier and much more versatile access to the current thiophene headgroups, however, allowed detailed SAR studies that were not available for the (+)-3-carene derived bicyclo[3.1.0]hexane fused thiophenes. For instance, the influence of the substituent in position 5 of the thiophene as well as of the two methyl groups attached to the cyclohexane ring could be studied easily. In the cyclohexane fused thiophene series, the 5-substituent strongly influenced the compound's affinity for the S1P₃ receptor. With increasing length of this alkyl chain the compounds became less selective for the S1P₁ receptor. For instance, attaching an *n*-propyl group to position 5 of the thiophene head furnished dual S1P₁/S1P₃ receptor agonists (e.g., **43**). The affinity for the S1P₃ receptor also increased with increasing size of the substituents attached to the cyclohexane ring, and the two diethyl substituted compounds **47** and **55** were the least selective representatives in the propanone and the oxadiazole series, respectively. These observations illustrate that the S1P₁ receptor is rather tolerant, while the S1P₃ receptor is much more sensitive toward changes in size and shape of the thiophene headgroup. As observed earlier,⁸⁴ the linker between the thiophene head and the phenyl

Table 8. Mesenteric Lymph and Plasma Exposure after Oral Administration of 10 mg/kg of Compounds 42, 104, 105, and 106 to Male Wistar Rats



Compd	R	log D _{7,4}	Plasma		Mesenteric Lymph		EC ₅₀ [nM] ^a	
			C _{max} ^b [ng/mL]	AUC _{0-t} ^c [ng/mL/h]	C _{max} ^a [ng/mL]	AUC _{0-t} ^c [ng/mL/h]	S1P ₁	S1P ₃
42		4.3	911 (6 h)	16600	8090 (3 h)	70500	4.6	8.9
104		5.4	376 (6.4 h)	1880	9050 (1.4 h)	31300	2.4	15
105		3.6	1490 (25 h)	34200	10000 (1 h)	29100	4.7	26
106		4.9	813 (8 h)	16300	9530 (0.75 h)	60400	1.4	5.8

^aEC₅₀ values as determined in a GTPγS assay using membranes of CHO cells expressing either S1P₁ or S1P₃. EC₅₀ values represent geometric mean values of at least three independent measurements in duplicate. All compounds behaved as full agonists on S1P₁ and S1P₃ ($E_{max} > 85\%$). For details see Experimental Section. ^bt_{max} given in parentheses. ^c0–t = from 0 h to last quantifiable measurement (t = 24 h except for **104**, t = 6.4 h).

ring bearing the polar side chain further influenced the compound's selectivity against the S1P₃ receptor. In general, the oxadiazole linked compounds were more potent on S1P₃ and thus less selective for S1P₁ than their propanone linked analogues. On the other hand, the oxadiazole derivatives usually showed lower in vitro and in vivo clearance and as a consequence a higher efficacy in sequestering lymphocytes from circulation. Several oxadiazole derivatives (e.g., **42**, **81**, **82**, and **84–87**) maximally reduced LC for at least 24 h after oral dosing of 10 mg/kg to Wistar rats. Among these, compounds **85** and **87** appear particularly interesting, as they incorporate a simple alkyl substituted thiophene head and combine high affinity and selectivity for S1P₁ with sustained maximal LC reduction.

Finally, we discovered that lymphatic transport is a significant route of absorption for several of the compounds discussed in this study. Compounds that undergo lymphatic transport may offer several advantages. First, although these compounds may ultimately end up in the systemic circulation, they avoid hepatic first pass metabolism. Lymphatic transport may therefore positively influence the bioavailability of a compound.^{100,101} Second, lymphatic transport may also offer opportunities for a tissue targeted approach wherein plasma exposure is minimal. The PKC inhibitor sotrastaurin, for instance, showed superior immunosuppressor efficacy in vivo when compared to a structurally close analogue reaching similar plasma exposure but lacking significant lymphatic absorption.¹⁰² Mesenteric lymph concentrations of compounds **42** and **104–106** exceeded those in plasma significantly. These compounds may therefore be particularly useful in diseases where mesenteric lymph represents the target compartment. This may indeed be the case for autoimmune diseases affecting the gastrointestinal tract such as ulcerative colitis or Crohn's disease. More detailed studies to understand the correlation between tissue specific pharmacokinetic behavior and efficacy in relevant disease models are certainly warranted for the compounds described above.

EXPERIMENTAL SECTION

Chemistry. All reagents and solvents were used as purchased from commercial sources (Sigma-Aldrich Switzerland, Lancaster Synthesis GmbH, Germany, Acros Organics USA). Moisture sensitive reactions were carried out under an argon atmosphere. Progress of the reactions was followed either by thin-layer chromatography (TLC) analysis (Merck, 0.2 mm silica gel 60 F₂₅₄ on glass plates) or by LC–MS. LC–MS parameters were the following: Finnigan MSQ Plus or MSQ surveyor (Dionex, Switzerland), with HP 1100 binary pump and DAD (Agilent, Switzerland); column Zorbax SB-AQ, 3.5 μm, 120 Å, 4.6 mm × 50 mm (Agilent) or Zorbax extended C18, 1.8 μm, 4.6 mm × 20 mm (Agilent); gradient, 5–95% acetonitrile in water containing 0.04% of trifluoroacetic acid, within 1 min; flow, 4.5 mL/min; 40 °C; t_R is given in min; UV detection at 230, 254, and 280 nm. LC–MS analysis was done on a Waters Acquity UPLC system equipped with an ACQ-PDA detector, an ACQ-ESL detector, and an ACQ-SQ detector; column ACQUITY UPLC BEH C18 1.7 μm, 2.1 mm × 50 mm; gradient, 2–98% acetonitrile containing 0.045% formic acid in water containing 0.05% formic acid over 1.8 min; flow, 1.2 mL/min; 60 °C.

HPLC Using Chiral Stationary Phase. Hardware from UltiMate instrument series (Dionex) and parameters were the following: HPG-3200SD binary pump, WPS-3000 autosampler, TCC-3200 thermostated column compartment, DAD-3000 detector, SRD-3400 degasser, ValveMate 2 (Gilson) solvent valves; column, solvent, and retention time (t_R) as indicated, DEA = diethylamine, TFA = trifluoroacetic acid, at 25 °C, flow 1 mL/min. No racemization was observed during the synthesis of the target compounds. LC–HRMS parameters were the following: analytical pump, Waters Acquity Binary Solvent Manager; MS, SYNAPT G2MS, source temperature 150 °C; desolvation temperature 400 °C; desolvation gas flow 400 L/h; cone gas flow, 10 L/h; extraction cone, 4 RF; lens, 0.1 V; sampling cone, 30; capillary, 1.5 kV; high resolution mode; gain, 1.0; MS function, 0.2 s per scan; 120–1000 amu in full scan, centroid mode; lock spray, leucine enkephalin 2 ng/mL (556.2771 Da); scan time 0.2 s with interval of 10 s and average of five scans; DAD, Acquity UPLC PDA detector; column: Acquity UPLC BEH C18 1.7 μm, 2.1 mm × 50 mm from Waters, thermostated in the Acquity UPLC column manager at 60 °C. Eluents were the following: water + 0.05% formic acid; B, acetonitrile + 0.05% formic acid. Gradient was 2–98% B over 3.0 min. Flow was 0.6 mL/min. Detection was with UV 214 nm and MS. t_R is given in min.

NMR Spectroscopy. Equipment used was Varian Oxford for ^1H (300 MHz) or ^{13}C (75 MHz) or Bruker Avance II, 400 MHz UltraShield, for ^1H (400 MHz) and ^{13}C (100 MHz). Chemical shifts are reported in parts per million (ppm) relative to tetramethylsilane (TMS), and multiplicities are given as s (singlet), d (doublet), t (triplet), q (quartet), quint (quintuplet), h (hexet), hept (heptuplet), m (multiplet), or br (broad). Coupling constants are given in Hz. Several compounds have been prepared in a combinatorial library format on a 15–50 mmol scale. For those compounds ^1H NMR spectra were acquired using nondeuterated 10 mM DMSO stock solutions submitted for biological testing.¹⁰³ The solvent and water signal were suppressed by irradiation at 2.54 and 3.54 ppm, respectively. As a consequence, signal integrals close to those frequencies are not always accurate. The numbers of protons given in the description represent observed values.

Compound Purification. Compounds were purified by flash column chromatography (CC) on silica gel 60 (Fluka Sigma-Aldrich, Switzerland) or by preparative HPLC (Waters XBridge Prep C18, 5 μm , OBD, 19 mm \times 50 mm, or Waters X-terra RP18, 19 mm \times 50 mm, 5 μm , gradient of acetonitrile in water containing 0.4% of formic acid, flow of 75 mL/min) or by MPLC (Labomatic MD-80-100 pump, linear UVIS-201 detector, column 350 mm \times 18 mm, Labogel-RP-18-5s-100, gradient of 10% methanol in water to 100% methanol).

X-ray Diffraction. To determine the molecular structure of thiophenecarboxylic acids **9**, **97**, and **103**, a crystal of the compound was mounted on a Bruker Nonius diffractometer equipped with a CCD detector and reflections were measured using monochromatic Mo K α radiation. The structure was solved by direct methods using SIR92. Refinement was performed with CRYSTALS. Full matrix least-squares refinement was performed with anisotropic temperature factors for all atoms except hydrogen which were included at calculated positions with isotropic temperature factors. Coordinates, anisotropic temperature factors, bond lengths, and bond angles have been deposited at the Cambridge Crystallographic Data Centre, 12 Union Road, Cambridge CB2 1EZ, United Kingdom, <http://www.ccdc.cam.ac.uk/>, under the following deposition numbers: 972174 (**9**), 972173 (**97**), 972175 (**103**).

Purity. The purity of all target compounds was assessed using the two independent LC–MS methods described above: (1) a Zorbax SB-AQ, 5 μm , 120 \AA , 4.6 mm \times 50 mm (Agilent) column, eluting with a gradient of 5–95% acetonitrile in water containing 0.04% of trifluoroacetic acid, within 1 min, flow of 4.5 mL/min, and (2) an ACQUITY UPLC BEH C18 1.7 μm , 2.1 mm \times 50 mm column, eluting with a gradient of 2–98% acetonitrile containing 0.045% formic acid in water containing 0.05% formic acid over 1.8 min, flow of 1.2 mL/min. In addition, important compounds were analyzed by LC–HRMS as described above. Purity and identity of the target compounds were further corroborated by NMR spectroscopy, and chiral integrity was proven by HPLC using chiral stationary phases. No racemization/epimerization was observed during the synthesis of the target compounds. According to these LC–MS analyses, final compounds showed a purity of $\geq 95\%$ (UV at 230 and at 214 nm).

In Vitro Potency Assessment. Data (EC_{50}) are given as geometric means (X_{geo}) with geometric standard deviation (σ_g). The upper and lower 95% confidence limits are calculated as $X_{\text{geo}}\sigma_g^2$ and $X_{\text{geo}}/\sigma_g^2$, respectively (results not shown).

GTP γ S Binding Assays. GTP γ S binding assays were performed in 96-well polypropylene microtiter plates in a final volume of 200 μL . Membrane preparations of CHO cells expressing recombinant human S1P $_1$ or S1P $_3$ receptors were used. Assay conditions were 20 mM Hepes, pH 7.4, 100 mM NaCl, 5 mM MgCl $_2$, 0.1% fatty acid free BSA, 1 or 3 μM GDP (for S1P $_1$ or S1P $_3$, respectively), 2.5% DMSO, and 50 pM ^{35}S -GTP γ S. Test compounds were dissolved and diluted and preincubated with the membranes, in the absence of ^{35}S -GTP γ S, in 150 μL of assay buffer at room temperature for 30 min. After addition of 50 μL of ^{35}S -GTP γ S in assay buffer, the reaction mixture was incubated for 1 h at room temperature. The assay was terminated by filtration of the reaction mixture through a multiscreen GF/C plate, prewetted with ice-cold 50 mM Hepes, pH 7.4, 100 mM NaCl, 5 mM MgCl $_2$, 0.4% fatty acid free BSA, using a cell harvester. The filter plates

were then washed with ice-cold 10 mM Na $_2$ HPO $_4$ /NaH $_2$ PO $_4$ (70%/30%, w/w) containing 0.1% fatty acid free BSA. Then the plates were dried at 50 $^\circ\text{C}$ and sealed. An amount of 25 μL of MicroScint20 was added, and membrane-bound ^{35}S -GTP γ S was determined on the TopCount. Specific ^{35}S -GTP γ S binding was determined by subtracting nonspecific binding (the signal obtained in the absence of agonist) from maximal binding (the signal obtained with 10 μM S1P). The EC_{50} of a test compound is the concentration of a compound inducing 50% of specific binding.

Metabolic Stability in Liver Microsomes and Hepatocytes.

Glucose 6-phosphate (disodium salt) and NADP were purchased from Sigma (Buchs, Switzerland). Glucose 6-phosphate dehydrogenase was supplied by Boehringer Mannheim (Rotkreuz, Switzerland). All other chemicals and solvents used throughout this study were of the highest commercially available quality. Liver microsomal preparations from humans (pool of 48 donors), male Wistar rat (pool of 4 animals), and Beagle dog (pool of several animals) were purchased from Becton Dickinson (Basel, Switzerland). They were employed at a microsomal protein concentration of 0.5 mg/mL. The NADPH-regenerating system used for the microsomal incubations was prepared as a 10-fold concentrated stock solution and kept at $-20\text{ }^\circ\text{C}$. It consisted of 11 mM NADP, 100 mM glucose 6-phosphate, and 50 mM MgCl $_2$ in 0.1 M phosphate buffer (pH 7.4). An amount of 20 UI/mL glucose 6-phosphate dehydrogenase was added before use. Incubations of compounds were performed at a single concentration of 1 μM in a total reaction volume of 1 mL at 37 $^\circ\text{C}$ in an Eppendorf thermomixer at 450 rpm. The reaction was initiated by addition of the NADPH-regenerating system (100 μL) containing the glucose 6-phosphate dehydrogenase and terminated after appropriate time periods up to 15 min by addition of ice-cold methanol (100 μL) to aliquots (100 μL) of the reaction mixture. The samples were centrifuged at 3220g for 20 min at 4 $^\circ\text{C}$, and an aliquot (10 μL) of the supernatant was submitted to LC–MS–MS analysis. The total concentration of DMSO in the assay did not exceed 0.1%. Male rat hepatocytes were prepared following the standard two-step collagenase perfusion method.¹⁰⁴ Freshly prepared hepatocytes were cultured in phenol red-free William's medium E supplemented with 10% fetal calf serum, 0.7 μM insulin, 10,000 UI/mL penicillin, and 10 mg/mL streptomycin (preincubation medium). Freshly isolated rat hepatocytes were centrifuged at 50g for 4 min at 4 $^\circ\text{C}$ and resuspended in preincubation medium, and the cell number and initial viability were determined using the erythrosine exclusion test. Cell viabilities below 85% were rejected for use. After a second centrifugation step, cells were resuspended in preincubation medium at a nominal density of 5.0×10^5 viable cells/mL. Aliquots (400 μL) of this suspension were dispensed into collagen-coated 24-well plates and incubated at 37 $^\circ\text{C}$ for a period of about 3 h in a humidified atmosphere containing 5% CO $_2$. At the end of the preincubation period, the medium was removed from each well and replaced with 200 μL of prewarmed (37 $^\circ\text{C}$) incubation medium containing compounds at a final concentration of 1 μM . Duplicate wells were sampled at 0, 0.5, 1, 2, 4, and 24 h by addition of 200 μL of methanol containing 0.3% SDS, and the entire well content was transferred into cryovials. Samples were stored frozen at $-20\text{ }^\circ\text{C}$ pending analysis. Compound disappearance was monitored by LC–MS–MS (MRM). Intrinsic clearances were determined by initial first order disappearance rates according to Obach et al.¹⁰⁵

Pharmacokinetics in the Rat. Male Wistar rats (RCC Ltd., Biotechnology and Animal Breeding Division, Füllinsdorf, Switzerland) were used for pharmacokinetic experiments after an acclimatization period of at least 7 days after delivery. The body weight of the rats was about 250 g at the day of the experiment. Two days prior to dosing, rats were anesthetized via inhalation by the gas anesthetic isoflurane. Buprenorphine was dosed as analgesic at 0.03 mg/kg sc half an hour before the operation. Catheters were implanted into the jugular vein and carotid artery under aseptic conditions to allow for multiple serial blood sampling. Animals foreseen for oral dosing did not undergo surgery, and blood samples were taken sublingually under light anesthesia with isoflurane. Compounds were administered intravenously as a 5 min infusion via the jugular vein at a dose of 1

mg/kg body weight formulated as solutions in an aqueous mixed micellar vehicle based on phospholipids and bile acids. Oral administration at a dose of 10 mg/kg was performed by gavage. For that, the compounds were dissolved in DMSO. This solution was added to a stirred solution of succinylated gelatin (7.5%) in water. The resulting milky suspension contained 5% of DMSO. Serial blood samples of 0.25 mL each were taken predose and at 30 min and 1, 2, 3, 4, 6, 8, and 24 h postdose into vials containing EDTA as anticoagulant. For the iv applications, additional samples were obtained 2, 10, and 20 min after the end of infusion. Plasma was separated by centrifugation and stored at $-20\text{ }^{\circ}\text{C}$. By use of $1.25\ \mu\text{L}$ of plasma on column, lower and upper limits of quantification were 1.52 and 1.52 ng/mL and 3300 and 10 000 ng/mL for compounds **36** and **42**, respectively. Pharmacokinetic parameters were estimated with the WinNonlin software (Pharsight Corporation, Mountain View, CA, USA) using noncompartmental analysis.

For lymph sampling, rats were put under anesthesia by 150 mg/kg thiobutobarbital sodium salt, ip, at selected times after oral dosing and a catheter was inserted into the thoracic lymph duct after a laparotomy. The mesenteric lymph was collected for at least 10 min. Also a blood sample was taken at the mean time of the lymph collection period. At the end of the sampling period rats were euthanized with pentobarbital (iv or ip). All animals had free access to food and water during the entire duration of the experiments. Plasma and lymph samples from the rat were analyzed after protein precipitation with methanol and centrifugation at 3220g for 20 min at $4\text{ }^{\circ}\text{C}$ using liquid chromatography coupled to mass spectrometry (LC-MS-MS) using appropriate calibration curves, internal standards (close analogues), and bioanalytical quality controls.

In vivo efficacy of the target compounds was assessed by measuring the circulating lymphocytes after oral administration of 1–10 mg/kg of a target compound to normotensive male Wistar rats. The animals were housed in climate-controlled conditions with a 12 h light/dark cycle and had free access to normal rat chow and drinking water. Blood was collected before and 3, 6, and 24 h after drug administration. Full blood was subjected to hematology using Beckman Coulter Ac-T Sdiff CP (Beckman Coulter International SA, Nyon, Switzerland). The effect on lymphocyte count (% LC) was calculated for each animal as the difference between LC at a given time point and the predose value (=100%). All data are presented as the mean \pm SEM. Statistical analyses were performed by analysis of variance (ANOVA) using Statistica (StatSoft) and the Student–Newman–Keuls procedure for multiple comparisons. Because of interindividual variability and the circadian rhythm of the number of circulating lymphocytes, a compound showing relative changes in the range of -20% to $+40\%$ is considered inactive. A lymphocyte count reduction in the range of -60% to -75% represents the maximal effect to be observed under the conditions of the experiment. The null hypothesis was rejected when $p < 0.05$. For formulation, the compounds were dissolved in DMSO. This solution was added to a stirred solution of succinylated gelatin (7.5%) in water. The resulting milky suspension containing a final concentration of 5% of DMSO was administered to the animals by gavage. A mixture of 95% of succinylated gelatin (7.5%) in water and 5% of DMSO served as vehicle.

5,5-Dimethyl-4,5,6,7-tetrahydrobenzo[c]thiophene-1-carboxylic Acid (8). (a) To a solution of 4,4-dimethylcyclohex-2-enone (50 g, 403 mmol) in EA (230 mL) a suspension of Pd/C (2.5 g, 10% Pd) in EA is added. The suspension is stirred at room temperature for 2 h under 1 bar of H_2 . The catalyst is filtered off and the solvent of the filtrate is carefully evaporated to give 4,4-dimethyl-cyclohexanone **5** (50 g, 98%) as a colorless oil which slowly crystallizes. $^1\text{H NMR}$ (CDCl_3): δ 2.34 (t, $J = 6.4\text{ Hz}$, 4 H), 1.66 (t, $J = 6.4\text{ Hz}$, 4 H), 1.09 (s, 6 H).

(b) To an ice-cold solution of potassium *tert*-butylate (24.5 g, 109 mmol, 50% solution in *tert*-butanol) in THF (700 mL), ethyl formate (120 mL, 123 mmol) is slowly added. The mixture is stirred at room temperature for 30 min before a solution of **5** (50 g, 396 mmol) in ethyl formate (50 mL) and THF (70 mL) is added over a period of 20 min. Upon complete addition, stirring is continued at $15\text{--}20\text{ }^{\circ}\text{C}$ for 30

min. The orange suspension is poured onto 10% aqueous citric acid solution (200 mL) and brine (200 mL) and extracted with EA ($2 \times 200\text{ mL}$). The organic extracts are washed with 0.2 N aqueous NaOH and brine, dried over Na_2SO_4 , and evaporated to dryness to give 5,5-dimethyl-2-oxocyclohexanecarbaldehyde **6** (52 g, 85%) as a yellow oil. LC-MS: $t_{\text{R}} = 0.89\text{ min}$, $[\text{M} + 1 + \text{CH}_3\text{CN}]^+ = 196.15$. $^1\text{H NMR}$ (CDCl_3): δ 14.42 (d, $J = 2.1\text{ Hz}$, 1 H), 8.59 (d, $J = 1.8\text{ Hz}$, 1 H), 2.40 (t, $J = 6.8\text{ Hz}$, 2 H), 2.14 (s, 2 H), 1.50 (t, $J = 6.8\text{ Hz}$, 2 H), 1.01 (s, 6 H).

(c) To a solution of **6** (51 g, 331 mmol) in chloroform (250 mL), oxalyl chloride (40 mL, 465 mmol) is rapidly added. Gas evolution is observed, and the mixture becomes warm ($35\text{ }^{\circ}\text{C}$). The mixture is cooled with a water bath to $20\text{--}25\text{ }^{\circ}\text{C}$. After the mixture was stirred for 1 h, ice followed by 3 N aqueous NaOH (100 mL) is added carefully. Again, gas formation is observed. The mixture is stirred for 45 min until gas evolution has ceased. The organic phase is separated, and the aqueous phase is extracted once more with chloroform. The combined organic extracts are washed with water and dried over Na_2SO_4 . The solvent is removed in vacuo to give crude 2-chloromethylene-4,4-dimethylcyclohexanone **7** (50 g, 87%) as a brown oil. LC-MS: $t_{\text{R}} = 0.96\text{ min}$. $^1\text{H NMR}$ (CDCl_3): δ 7.15 (t, $J = 2.1\text{ Hz}$, 1 H), 2.47 (t, $J = 7.0\text{ Hz}$, 2 H), 2.43 (s, 2 H), 1.71 (t, $J = 7.0\text{ Hz}$, 2 H), 1.06 (s, 6 H).

(d) To a part (300 mL) of a freshly prepared solution of sodium (21 g, 875 mmol) in ethanol (500 mL), mercaptoacetic acid ethyl ester (50 mL) is added. The resulting solution is added over a period of 10 min to a solution of **7** (50 g, 290 mmol) in THF (170 mL). The mixture becomes warm ($50\text{ }^{\circ}\text{C}$). Upon complete addition, the remaining part of the freshly prepared solution of sodium in ethanol (200 mL) is added to the reaction mixture. The mixture is stirred at room temperature for 15 min before 1 N aqueous LiOH solution (300 mL) is added. The solution is refluxed for 3 h, then stirred at room temperature for 16 h. The THF and ethanol are removed under reduced pressure, and the remaining dark solution is extracted with heptane/EA 3:1 ($2 \times 200\text{ mL}$). The aqueous phase is acidified by adding citric acid (30 g) and 2 N aqueous HCl (200 mL) and then extracted three times with EA. The combined organic extracts are washed three times with saturated aqueous NaHCO_3 solution, dried over Na_2SO_4 , and evaporated. The resulting dark brown oil is dissolved in acetonitrile at $60\text{ }^{\circ}\text{C}$ and crystallized at $5\text{ }^{\circ}\text{C}$. The crystals are collected, washed with acetonitrile, and dried to give **8** (31 g, 51%) as a slightly gray powder. LC-MS: $t_{\text{R}} = 0.95\text{ min}$, $[\text{M} + 1 + \text{CH}_3\text{CN}]^+ = 252.18$. $^1\text{H NMR}$ (CDCl_3): δ 7.15 (s, 1 H), 3.05 (t, $J = 7.0\text{ Hz}$, 2 H), 2.47 (s, 2 H), 1.58 (t, $J = 7.0\text{ Hz}$, 2 H), 0.97 (s, 6 H).

3,5,5-Trimethyl-4,5,6,7-tetrahydrobenzo[c]thiophene-1-carboxylic Acid (9). At $-78\text{ }^{\circ}\text{C}$ a solution of **8** (5 g, 23.8 mmol) in THF is treated with *tert*-butyllithium (41 mL, 1.5 M in pentane). The mixture is stirred at $-78\text{ }^{\circ}\text{C}$ for 15 min before methyl iodide (17.1 g, 120 mmol) is added dropwise. Stirring is continued at $-78\text{ }^{\circ}\text{C}$ for 30 min. The mixture is warmed to room temperature, diluted with water (400 mL), acidified with 10% aqueous citric acid solution, and extracted three times with EA. The combined organic extracts are dried over MgSO_4 and evaporated. The remaining solid is suspended in heptane/diethyl ether, filtered, and dried under HV to give **9** (4.01 g, 75%) as a beige powder. LC-MS: $t_{\text{R}} = 0.97\text{ min}$, $[\text{M} + 1] = 225.13$. $^1\text{H NMR}$ ($\text{DMSO}-d_6$): δ 12.49 (s br, 1 H), 2.87 (t, $J = 6.7\text{ Hz}$, 2 H), 2.26 (s, 5 H), 1.45 (t, $J = 6.7\text{ Hz}$, 2 H), 0.91 (s, 6 H). $^{13}\text{C NMR}$ ($\text{DMSO}-d_6$): δ 164.0, 145.4, 139.1, 136.4, 122.7, 38.3, 35.3, 29.6, 28.1, 24.2, 13.4. Crystals suitable for single crystal X-ray structure analysis were obtained by crystallizing **9** from acetonitrile. Crystals of **9** ($\text{C}_{12}\text{H}_{16}\text{O}_2\text{S}$, formula weight 224.09) formed in the triclinic space group $\text{P}\bar{1}$. A total of 12 337 reflections was measured at 293 K. Results were the following: molecules/unit cell $Z = 2$, cell dimensions $a = 6.6024(6)\text{ \AA}$, $b = 8.6950(8)\text{ \AA}$, $c = 9.8154(10)\text{ \AA}$, $\alpha = 96.056(7)^\circ$, $\beta = 96.461(7)^\circ$, $\gamma = 94.944(6)^\circ$; calculated density of 1.34 g cm^{-3} . The final R -factor of 0.031 was obtained for 2416 observed reflections ($I > 3\sigma(I)$). CCDC code is 972174.

3-Ethyl-5,5-dimethyl-4,5,6,7-tetrahydrobenzo[c]thiophene-1-carboxylic Acid (10). To a cooled solution ($-78\text{ }^{\circ}\text{C}$) of **8** (960 mg, 4.57 mmol) in THF (19 mL), *tert*-butyllithium (8 mL, 1.5 M

solution in pentane) is added. The mixture is stirred at -78°C for 10 min before ethyl iodide (3.80 g, 24.37 mmol) is added. The reaction mixture is stirred at -78°C for 3 h. Water/methanol 1:1 (8 mL) followed by 10% aqueous citric acid solution is added, and the mixture is extracted with EA. The combined organic extracts are washed with brine, dried over Na_2SO_4 , and evaporated. The remaining solid is suspended in acetonitrile (6 mL), heated to 60°C , cooled to room temperature, filtered, and dried to give **10** (640 mg, 50%) as a slightly beige solid. LC-MS: $t_{\text{R}} = 1.01$ min, $[\text{M} + 1 + \text{CH}_3\text{CN}] = 280.10$. ^1H NMR ($\text{DMSO}-d_6$): δ 12.48 (s br, 1 H), 2.87 (t, $J = 6.8$ Hz, 2 H), 2.66 (q, $J = 7.5$ Hz, 2 H), 2.27 (s, 2 H), 1.46 (t, $J = 6.7$ Hz, 2 H), 1.15 (t, $J = 7.5$ Hz, 3 H), 0.91 (s, 6 H). ^{13}C NMR (CDCl_3): δ 168.6, 149.23, 149.21, 134.6, 121.4, 40.8, 35.3, 29.5, 28.0, 21.9, 21.5, 14.7.

1-(3,5,5-Trimethyl-4,5,6,7-tetrahydrobenzo[*c*]thiophen-1-yl)ethanone (14). To a suspension of **9** (4.10 g, 18.28 mmol) in diethyl ether (300 mL), methyl lithium (23 mL, 1.6 M solution in diethyl ether) is slowly added at room temperature. The reaction mixture becomes clear, yellow, and slightly warm (26°C) and is stirred for 15 min before it is quenched with water. The organic layer is separated, washed once more with water, dried over MgSO_4 , and evaporated. The crude product is purified by CC on silica gel, eluting with heptane/EA 4:1 to give **14** (2.80 g, 69%) as a pale yellow crystalline solid. LC-MS: $t_{\text{R}} = 0.97$ min, $[\text{M} + 1] = 223.26$. ^1H NMR (CDCl_3): δ 3.00 (t, $J = 7.0$ Hz, 2 H), 2.43 (s, 3 H), 2.31 (s, 3 H), 2.26 (s, 2 H), 1.51 (t, $J = 7.0$ Hz, 2 H), 0.95 (s, 6 H). ^{13}C NMR (CDCl_3): δ 190.6, 145.6, 140.0, 137.3, 131.7, 38.6, 35.4, 29.4, 27.9, 25.2, 13.5.

4-Isobutyl-3-methylthiophene-2-carboxylic Acid (94). (a) To a solution of KO^tBu (50 g, 446 mmol) in THF (400 mL) is added during 30 min ethyl formate (92 g, 1.25 mol). Strong gas evolution occurs. The mixture is cooled during the addition with a water bath at 10°C . After complete addition, the mixture is stirred until the gas evolution ceases (15 min). The mixture is cooled with ice at 0°C , and a mixture of 5-methyl-2-hexanone **91** (34.25 g, 300 mmol) and ethyl formate (41 g, 0.55 mol) is added slowly during 30 min. The mixture is stirred for 15 h, diluted with EA (500 mL), and washed with 1 N aqueous HCl (100 mL), 1 M aqueous NaH_2PO_4 solution (100 mL), and brine (100 mL). The organic extract is dried (MgSO_4), filtered, and evaporated to give crude 4-hydroxy-3-isobutylbut-3-en-2-one **92** (28 g, 66%) which is used without further purification. LC-MS: $t_{\text{R}} = 0.80$ min, $[\text{M} + 1] = 143.39$. ^1H NMR (CDCl_3): δ 7.99 (d, $J = 6.4$ Hz, 1 H), 2.11 (s, 3 H), 2.00 (d, $J = 7.2$ Hz, 2 H), 1.60 (hept, $J = 7.0$ Hz, 1 H), 0.89 (d, $J = 6.6$ Hz, 6 H).

(b) To a solution of **92** (28 g, 197 mmol) in chloroform (350 mL) a solution of oxalyl chloride (44.3 g, 349 mmol) in chloroform (50 mL) is added slowly during 5 min. The resulting dark brown mixture is stirred at room temperature for 2 h before it is cooled to 0°C and treated with ice (100 g) followed by 1 N aqueous NaOH (100 mL). When the quite violent gas evolution ceases, the phases are separated (the still acidic aqueous phase is discarded). The organic phase is washed with 1 N aqueous NaOH (3 \times 75 mL) and 1 N aqueous NaH_2PO_4 (75 mL), dried (MgSO_4), filtered, and evaporated to give crude 4-chloro-3-isobutylbut-3-en-2-one **93** (31.6 g, quantitative) as a dark brown oil. LC-MS: $t_{\text{R}} = 0.97$ min. ^1H NMR (CDCl_3): δ 7.29 (s, 1 H), 2.36 (d, $J = 7.3$ Hz, 2 H), 2.31 (s, 3 H), 1.81 (hept, $J = 6.8$ Hz, 1 H), 0.87 (d, $J = 6.7$ Hz, 6 H).

(c) KO^tBu (44.2 g, 394 mmol) is added portionwise to ethanol (200 mL). The mixture is stirred for 30 min at 20°C to dissolve all KO^tBu . Mercaptoacetic acid ethyl ester (47.3 g, 394 mmol) is added, and the temperature is maintained at 20°C . This solution is slowly added at 20°C to a solution of the crude **93** (31.6 g, 197 mmol) in THF (350 mL). The mixture is stirred at room temperature for 15 h before sodium ethylate (13.4 g, 197 mmol) is added, and stirring is continued at reflux for 1 h. The mixture is cooled to room temperature, and the solvents are evaporated on a rotavap. The residue is diluted with diethyl ether (500 mL), washed with 1 M aqueous NaH_2PO_4 (200 mL), 1 N aqueous NaOH (2 \times 100 mL), saturated aqueous NaHCO_3 (35 mL) containing 10% aqueous NaOCl (15 mL), and brine (100 mL), dried over Na_2SO_4 , filtered, and evaporated. The resulting residue (36.3 g) is dissolved in EtOH (250 mL). 2 N aqueous LiOH (100 mL) is added, and the mixture is stirred

at room temperature for 48 h before it is extracted with diethyl ether (1 \times 400 mL, 2 \times 150 mL). The organic extracts are washed with 1 N aqueous NaOH (3 \times 100 mL). The aqueous extracts are carefully acidified with 25% aqueous HCl and then extracted with DCM (3 \times 150 mL). The combined DCM extracts are dried over MgSO_4 , filtered, and evaporated. The crude product is purified by crystallization from acetonitrile (150 mL) at 4°C to give **94** (16.0 g, 41%) as a beige-brown crystalline powder. LC-MS: $t_{\text{R}} = 0.95$ min. ^1H NMR (CD_3OD): δ 7.21 (s, 1 H), 2.43 (s, 3 H), 2.42 (d, $J = 7.0$ Hz, 2 H), 1.83 (nonet, $J = 7.0$ Hz, 1 H), 0.92 (d, $J = 7.0$ Hz, 6 H).

4-Isobutyl-5-methylthiophene-2-carboxylic Acid (96). (a) Phosphorus oxychloride (53.7 g, 350 mmol) is slowly added to DMF (60 mL) stirred at 5°C . Upon complete addition, the clear solution is stirred for further 30 min at 5°C before 5-methyl-2-hexanone **91** (20 g, 175 mmol) is added dropwise. The yellow solution is stirred for 30 min at 0°C , then for 90 min at room temperature. The mixture becomes warm (40°C), and a thick suspension forms. The mixture is cooled to 25°C , and stirring is continued for 1 h before it is poured into an aqueous solution of NaOAc (80 g)/ice mixture. The mixture is extracted twice with diethyl ether. The organic extracts are washed with water, combined, dried over MgSO_4 , filtered, and evaporated to give crude 3-chloro-2-isobutylbut-2-enal **95** (35.4 g, quantitative) as a 2:3 mixture of *E/Z* isomers as a yellow oil. LC-MS: $t_{\text{R}} = 0.97$ min. ^1H NMR (CDCl_3): δ major isomer 10.02 (s, 1 H), 2.60 (s, 3 H), 2.33 (d, $J = 7.3$ Hz, 2 H), 1.82 (hept, $J = 7.0$ Hz, 1 H), 0.87 (d, $J = 6.7$ Hz, 6 H); δ minor isomer 10.22 (s, 1 H), 2.38 (s, 3 H), 2.20 (d, $J = 7.3$ Hz, 2 H), 1.69 (hept, $J = 6.4$ Hz, 1 H), 0.86 (d, $J = 6.7$ Hz, 6 H).

(b) Sodium (10.7 g, 467 mmol) is dissolved in ethanol (500 mL), and the resulting solution is diluted with THF (100 mL) before mercaptoacetic acid ethyl ester (33.7 g, 280 mmol) dissolved in THF (70 mL) is slowly added at 5°C . The mixture is stirred at room temperature for 1 h before a solution of **95** (30 g, 187 mmol) in THF (100 mL) is slowly added at 8°C . The resulting yellow suspension is stirred at room temperature for 16 h. The reaction mixture is diluted with diethyl ether (500 mL) and is washed with dilute aqueous NaOCl solution followed by aqueous 1 N HCl and water. The organic extract is dried over MgSO_4 , filtered, and evaporated. The remaining orange oil is dissolved in ethanol (150 mL), and 2 N aqueous LiOH (50 mL) is added. The mixture is stirred for 16 h at 50°C , acidified with 2 N aqueous HCl, and extracted with EA. The organic extract is dried over MgSO_4 , filtered, and evaporated. The crude product is recrystallized from EA/heptane to give **96** (10.5 g, 28%) as colorless crystals. LC-MS: $t_{\text{R}} = 0.92$ min, $[\text{M} + 1 + \text{CH}_3\text{CN}] = 240.16$. ^1H NMR (CDCl_3): δ 7.59 (s, 1 H), 2.40–2.37 (m, 5 H), 1.84 (hept, $J = 7.0$ Hz, 1 H), 0.90 (d, $J = 7.0$ Hz, 6 H). ^{13}C NMR (CDCl_3): δ 167.8, 144.0, 139.3, 137.4, 127.4, 37.3, 29.6, 22.4, 14.0.

4-Isobutyl-3,5-dimethylthiophene-2-carboxylic Acid (97). Under argon, a solution of **96** (2.00 g, 10.1 mmol) in THF (150 mL) is allowed to stand over 3 Å molecular sieves for 30 min before it is transferred to the reaction vessel. The solution is cooled to -78°C , and $^t\text{BuLi}$ (20.2 mL of 1.5 M solution in pentane) is added. Upon complete addition, stirring is continued at -78°C for 45 min before MeI (7.16 g, 50.4 mmol) is added. Stirring is continued at -70°C for 30 min. The mixture is allowed to warm to room temperature. The reaction is quenched by adding 10% aqueous citric acid solution and water. The mixture is extracted three times with EtOAc (3 \times 200 mL). The organic extracts are combined, dried over MgSO_4 , filtered, and concentrated. The crude product is purified by column chromatography on silica gel, eluting with heptane/EtOAc 4:1 to give **97** (1.40 g, 65%) as a white solid. LC-MS: $t_{\text{R}} = 0.97$ min, $[\text{M} + 1 + \text{CH}_3\text{CN}] = 254.26$. ^1H NMR (CDCl_3): δ 2.46 (s, 3 H), 2.39 (s, 3 H), 2.36 (d, $J = 7.0$ Hz, 2 H), 1.78 (hept, $J = 7.0$ Hz, 1 H), 0.91 (d, $J = 7.0$ Hz, 6 H). ^{13}C NMR (CDCl_3): δ 168.7, 148.0, 142.3, 139.9, 122.2, 36.0, 29.2, 22.5, 14.9, 14.5. Crystals suitable for single crystal X-ray structure analysis were obtained by crystallizing **97** by the isothermal distillation method^{106,107} using EA as solvent and hexane as the precipitating agent. Crystals of **97** ($\text{C}_{11}\text{H}_{16}\text{O}_2\text{S}$, formula weight 212.09) formed in the monoclinic space group $\text{C}2/c$, and 13 680 reflections were measured at 293 K. Results were the following: molecules/unit cell

$Z = 8$, cell dimensions $a = 15.852(3)$ Å, $b = 7.0898(10)$ Å, $c = 20.177(3)$ Å, $\alpha = 90^\circ$, $\beta = 93.945(16)^\circ$, $\gamma = 90^\circ$; calculated density of 1.24 g cm $^{-3}$. The final R -factor of 0.035 was obtained for 2450 observed reflections ($I > 3\sigma(I)$). CCDC code is 972173 .

5-Isobutylthiophene-2-carboxylic Acid (102). To a solution of thiophene-2-carboxylic acid **98** (4.16 g, 32.1 mmol) in THF (200 mL) *tert*-butyllithium (49 mL, 1.7 M solution in pentane, 83.6 mmol) is slowly added at -78°C . The mixture is stirred at -78°C for 30 min before isobutyl bromide (22.7 g, 160.7 mmol) is carefully added. The mixture is stirred at -78°C for 5 h, then at room temperature for 16 h. The reaction is quenched by the addition of water (400 mL). The mixture is acidified and extracted with EA. The organic extract is dried over MgSO_4 , filtered, and evaporated. The crude product is purified by MPLC on reverse phase silica gel to give **102** (1.67 g, 28%) as a brownish oil. LC–MS: $t_{\text{R}} = 0.91$ min. $^1\text{H NMR}$ (CDCl_3): δ 7.73 (d, $J = 3.8$ Hz, 1 H), 6.80 (d, $J = 3.8$ Hz, 1 H), 2.72 (d, $J = 7.0$ Hz, 2 H), 1.94 (hept, $J = 6.7$ Hz, 1H), 0.96 (d, $J = 6.7$ Hz, 6 H). $^{13}\text{C NMR}$ (CDCl_3): δ 168.0, 154.5, 135.2, 130.3, 126.4, 39.8, 30.7, 22.2.

rac-N-(3-(2,6-Dimethyl-4-(3-oxo-3-(3,5,5-trimethyl-4,5,6,7-tetrahydrobenzo[c]thiophen-1-yl)propyl)phenoxy)-2-hydroxypropyl)-2-hydroxyacetamide (3). A solution of glycolic acid (61 mg, 0.806 mmol), TBTU (224 mg, 0.698 mmol), and Hünig's base (278 mg, 2.15 mmol) in DCM (5 mL) is stirred at room temperature for 10 min before a solution of **29** (231 mg, 0.537 mmol) in DCM (5 mL) is added. The mixture is stirred at room temperature for 1 h. Another portion of glycolic acid (61 mg, 0.806 mmol) and TBTU (100 mg, 0.311 mmol) is added, and stirring is continued for 2 h. The mixture is diluted with DCM and washed with saturated aqueous NaHCO_3 solution. The washing is extracted back two times with DCM. The organic extracts are combined, dried over MgSO_4 , filtered, and concentrated. The crude product is purified on preparative TLC plates using DCM containing 5% of methanol to give **3** (143 mg, 55%) as a colorless foam. LC–MS: $t_{\text{R}} = 1.00$ min, $[\text{M} + 1]^+ = 488.17$. HPLC with chiral stationary phase (Chiralpak IA 250 mm \times 4.6 mm i.d., 5 μm ; 90% heptane containing 0.05% DEA, 10% ethanol containing 0.05% DEA): $t_{\text{R}} = 19.7$ min, 48%, $t_{\text{R}} = 22.0$ min, 52%. $^1\text{H NMR}$ (CDCl_3): δ 6.97 (t br, $J = 5.0$ Hz, 1 H), 6.87 (s, 2 H), 4.08–4.15 (m, 1 H), 4.15 (s, 2 H), 3.69–3.84 (m, 3 H), 3.40–3.52 (m, 1 H), 2.97–3.08 (m, 4 H), 2.86–2.96 (m, 2 H), 2.33 (s, 3 H), 2.28 (s, 2 H), 2.24 (s, 6 H), 1.53 (t, $J = 6.7$ Hz, 2 H), 0.97 (s, 6 H). $^{13}\text{C NMR}$ (CDCl_3): δ 192.3, 172.9, 153.2, 146.0, 139.9, 137.3, 137.1, 131.0, 130.5, 129.0, 73.4, 70.2, 62.2, 43.5, 42.3, 38.6, 35.4, 30.0, 29.5, 27.9, 25.3, 16.3, 13.5. LC–HRMS: $t_{\text{R}} = 2.08$ min, $[\text{M} + \text{H}]^+/z = 488.2471$, found = 488.2470.

3-(4-Hydroxy-3,5-dimethyl-phenyl)-1-(3,5,5-trimethyl-4,5,6,7-tetrahydro-benzo[c]thiophen-1-yl)-propan-1-one (21). (a) A solution of 1-(3,5,5-trimethyl-4,5,6,7-tetrahydrobenzo[c]thiophen-1-yl)ethanone **14** (1.35 g, 6.07 mmol) and 4-hydroxy-3,5-dimethylbenzaldehyde (1.09 g, 7.29 mmol) in ethanol (20 mL) and 5 N HCl in isopropanol (10 mL) is stirred at room temperature for 100 min. The dark solution is diluted with diethyl ether (300 mL), washed with water followed by a 1:1 mixture of 1 N aqueous NaOH and saturated aqueous NaHCO_3 , dried over MgSO_4 , and evaporated. The crude product is purified by CC on silica gel, eluting with heptane/EA 7:3 to give 3-(4-hydroxy-3,5-dimethylphenyl)-1-(3,5,5-trimethyl-4,5,6,7-tetrahydrobenzo[c]thiophen-1-yl)propanone (1.86 g, 87%) as a yellow-orange solid. LC–MS: $t_{\text{R}} = 1.15$ min, $[\text{M} + 1] = 355.26$. $^1\text{H NMR}$ (CDCl_3): δ 7.65 (d, $J = 15.2$ Hz, 1 H), 7.26 (s, 2 H), 7.13 (d, $J = 15.2$ Hz, 1 H), 5.04 (s, 1 H), 3.15 (t, $J = 6.4$ Hz, 2 H), 2.37 (s, 3 H), 2.31 (s, 2 H), 2.28 (s, 6 H), 1.56 (t, $J = 6.4$ Hz, 2 H), 0.99 (s, 6 H).

(b) A solution of 3-(4-hydroxy-3,5-dimethylphenyl)-1-(3,5,5-trimethyl-4,5,6,7-tetrahydrobenzo[c]thiophen-1-yl)propanone (1.86 g, 5.25 mmol) in THF (50 mL) and ethanol (50 mL) is treated with Pd/C (400 mg, 10% Pd), and the resulting slurry is stirred at room temperature for 5 h under 1.5 bar of H_2 . The catalyst is filtered off, and the solvent of the filtrate is evaporated. The crude product is purified by CC on silica gel, eluting with heptane/EA 1:1 to give **21** (1.80 g, 96%) as a pale red foam. LC–MS: $t_{\text{R}} = 1.15$ min, $[\text{M} + 1] = 357.27$. $^1\text{H NMR}$ (CDCl_3): δ 6.85 (s, 2 H), 4.53 (s, 1 H), 3.07–2.98 (m, 4 H), 2.94–2.86 (m, 2 H), 2.33 (s, 3 H), 2.28 (s, 2 H), 2.22 (s, 6 H), 1.53 (t, $J = 7.0$ Hz, 2 H), 0.97 (s, 6 H). $^{13}\text{C NMR}$ (CDCl_3): δ

192.5, 150.5, 145.9, 139.7, 137.3, 132.9, 131.1, 128.5, 123.0, 43.9, 38.6, 35.5, 30.0, 29.5, 27.9, 25.3, 16.0, 13.5.

rac-3-[4-(3-Amino-2-hydroxypropoxy)-3,5-dimethylphenyl]-1-(3,5,5-trimethyl-4,5,6,7-tetrahydrobenzo[c]thiophen-1-yl)-propan-1-one (29). (a) To a solution of **21** (420 mg, 1.18 mmol) in isopropanol (15 mL) and 3 N aqueous NaOH (6 mL) *rac*-epichlorohydrin (545 mg, 5.89 mmol) is added. The mixture is stirred at room temperature for 20 h before it is diluted with diethyl ether (150 mL) and washed with saturated NaHCO_3 solution (50 mL). The washing is extracted back with diethyl ether (150 mL). The combined organic extracts are dried over MgSO_4 , filtered, and concentrated. The crude product is purified by column chromatography on silica gel, eluting with heptane/EtOAc 4:1 to give *rac*-3-(3,5-dimethyl-4-(oxiran-2-ylmethoxy)phenyl)-1-(3,5,5-trimethyl-4,5,6,7-tetrahydrobenzo[c]thiophen-1-yl)propan-1-one (443 mg, 91%) as an almost colorless oil. LC–MS: $t_{\text{R}} = 1.19$ min, $[\text{M} + 1]^+ = 413.36$. $^1\text{H NMR}$ (CDCl_3): δ 6.87 (s, 2 H), 4.00 (dd, $J_1 = 11.1$ Hz, $J_2 = 3.3$ Hz, 1 H), 3.73 (dd, $J_1 = 11.1$ Hz, $J_2 = 5.9$ Hz, 1 H), 3.31–3.39 (m, 1 H), 2.98–3.08 (m, 4 H), 2.85–2.96 (m, 3 H), 2.70 (dd, $J_1 = 4.9$ Hz, $J_2 = 2.6$ Hz, 1 H), 2.33 (s, 3 H), 2.28 (s, 2 H), 2.26 (s, 6 H), 1.53 (t, $J = 6.7$ Hz, 2 H), 0.97 (s, 6 H).

(b) A solution of the above epoxide (443 mg, 1.07 mmol) in 7 N NH_3 in methanol (15 mL) is stirred at 65°C for 18 h in a sealed vessel. The mixture is concentrated and dried to give **29** (443 mg, 96%) as a pale yellow foam. LC–MS: $t_{\text{R}} = 0.89$ min, $[\text{M} + 1]^+ = 430.33$. $^1\text{H NMR}$ ($\text{DMSO}-d_6$, solvent suppression): δ 6.87 (s, 2 H), 3.90–3.97 (m, 1 H), 3.63–3.65 (m, 1 H), 2.87–2.93 (m, 2 H), 2.73–2.82 (m, 2 H), 2.30 (s, 3 H), 2.27 (s, 2 H), 2.17 (s, 6 H), 1.43–1.50 (m, 2 H), 0.92 (s, 6 H).

rac-N-(3-[2-Ethyl-4-[3-(3-ethyl-5,5-dimethyl-4,5,6,7-tetrahydrobenzo[c]thiophen-1-yl)-3-oxopropyl]-6-methylphenoxy]-2-hydroxypropyl)-2-hydroxyacetamide (36). **36** was prepared in analogy to **3** using **15**, giving a beige foam. LC–MS: $t_{\text{R}} = 1.05$ min, $[\text{M} + 1] = 516.42$. HPLC with chiral stationary phase (Chiralpak IE 250 mm \times 4.6 mm i.d., 5 μm ; 70% heptane containing 0.05% DEA, 30% ethanol containing 0.05% DEA): $t_{\text{R}} = 11.0$ min, 50%, $t_{\text{R}} = 11.8$ min, 50%. $^1\text{H NMR}$ (CDCl_3): δ 6.86–6.95 (m, 3 H), 4.16 (s, 2 H), 4.09–4.15 (m, 1 H), 3.69–3.84 (m, 3 H), 3.40–3.52 (m, 1 H), 3.20 (s br, 1 H), 3.00–3.10 (m, 4 H), 2.90–2.98 (m, 2 H), 2.72 (q, $J = 7.6$ Hz, 2 H), 2.61 (q, $J = 7.5$ Hz, 2 H), 2.30 (s, 2 H), 2.25 (s, 3 H), 1.54 (t, $J = 7.0$ Hz, 2 H), 1.26 (t, $J = 7.6$ Hz, 3 H), 1.21 (t, $J = 7.8$ Hz, 3 H), 0.97 (s, 6 H). $^{13}\text{C NMR}$ (CDCl_3): δ 192.4, 172.8, 152.7, 147.6, 146.1, 137.4, 136.6, 136.4, 130.9, 130.5, 129.0, 127.2, 74.0, 70.2, 62.2, 43.5, 42.2, 38.6, 35.6, 30.2, 29.5, 27.9, 25.3, 22.9, 21.7, 16.4, 15.0, 14.9. LC–HRMS: $t_{\text{R}} = 2.25$ min, $[\text{M} + \text{H}]^+/z = 516.2784$, found = 516.2787.

N-((S)-3-[2-Ethyl-4-[5-(3-ethyl-5,5-dimethyl-4,5,6,7-tetrahydrobenzo[c]thiophen-1-yl)[1,2,4]oxadiazol-3-yl]-6-methylphenoxy]-2-hydroxypropyl)-2-hydroxyacetamide (42). (a) To a solution of **10** (2.00 g, 8.39 mmol) in DMF (25 mL) Hünig's base (2.17 g, 16.8 mmol) followed by TBTU (2.96 g, 9.23 mmol) is added. The mixture is stirred at room temperature for 10 min before 3-ethyl-4, *N*-dihydroxy-5-methylbenzamidine (1.63 g, 8.39 mmol, Supporting Information) is added. Stirring is continued at room temperature for 18 h. The mixture is diluted with EA and washed with water. The organic extract is dried over MgSO_4 , filtered, and concentrated. The residue is dissolved in dioxane (20 mL) and stirred under reflux for 20 h. The mixture is cooled to room temperature and concentrated, and the crude product is purified by CC on silica gel, eluting with heptane/EA 9:1 to give 2-ethyl-4-(5-(3-ethyl-5,5-dimethyl-4,5,6,7-tetrahydrobenzo[c]thiophen-1-yl)-1,2,4-oxadiazol-3-yl)-6-methylphenol (2.36 g, 71%) as a yellow solid. LC–MS: $t_{\text{R}} = 1.16$ min, $[\text{M} + 1] = 396.16$. $^1\text{H NMR}$ (CDCl_3): δ 7.82 (s, 2 H), 7.28 (s, 1 H), 4.99 (s, 1 H), 3.17 (t, $J = 6.8$ Hz, 2 H), 2.80 (q, $J = 7.5$ Hz, 2 H), 2.72 (q, $J = 7.6$ Hz, 2 H), 2.38 (s, 2 H), 2.35 (s, 3 H), 1.66 (t, $J = 6.7$ Hz, 2 H), 1.33 (t, $J = 7.5$ Hz, 3 H), 1.32 (t, $J = 7.3$ Hz, 3 H).

(b) The title compound is then prepared from the above phenol following the procedures described for compounds **3** and **29**, giving a white solid. LC–MS: $t_{\text{R}} = 1.05$ min, $[\text{M} + 1] = 528.23$. $^1\text{H NMR}$ (CDCl_3): δ 7.85 (s, 1 H), 7.84 (s, 1 H), 7.08 (t br, $J = 5.8$ Hz, 1 H), 4.18–4.24 (m, 3 H), 3.90 (dd, $J_1 = 9.6$ Hz, $J_2 = 4.6$ Hz, 1 H), 3.76–3.86 (m, 2 H), 3.48–3.56 (m, 1 H), 3.16 (t, $J = 6.7$ Hz, 2 H), 2.80 (q, J

= 7.5 Hz, 3 H), 2.74 (q, J = 7.5 Hz, 2 H), 2.38 (s, 5 H), 1.66 (t, J = 6.7 Hz, 2 H), 1.33 (t, J = 7.5 Hz, 3 H), 1.31 (t, J = 7.5 Hz, 3 H), 1.04 (s, 6 H). ^{13}C NMR (CDCl_3): δ 173.3, 172.2, 168.0, 157.0, 147.7, 144.7, 137.4, 135.7, 131.4, 128.4, 126.7, 123.1, 115.2, 74.1, 70.1, 62.2, 42.3, 38.5, 35.4, 29.6, 27.9, 24.3, 22.9, 21.6, 16.5, 14.91, 14.87. LC–HRMS: t_{R} = 2.47 min, $[\text{M} + \text{H}]^+ / z = 528.2532$, found = 528.2523.

rac-2-Hydroxy-*N*-(2-hydroxy-3-[(4-[(5-isobutylthiophen-2-yl)[1,2,4]oxadiazol-3-yl]-2,6-dimethylphenoxy)propyl]acetamide (87). 87 was prepared in analogy to 42 using 102, giving a white solid. LC–MS: t_{R} = 1.01 min, $[\text{M} + 1]^+ = 460.18$. ^1H NMR δ : 7.83 (s, 2 H), 7.80 (d, J = 3.7 Hz, 1 H), 7.00 (t br, J = 6.5 Hz, 1 H), 6.90 (d, J = 3.7 Hz, 1 H), 4.17–4.25 (m, 3 H), 3.90 (dd, J_1 = 9.5 Hz, J_2 = 4.5 Hz, 1 H), 3.83 (dd, J_1 = 9.5 Hz, J_2 = 6.3 Hz, 1 H), 3.76–3.83 (m, 1 H), 3.48–3.57 (m, 1 H), 2.79 (d, J = 7.1 Hz, 2 H), 2.37 (s, 6 H), 1.93–2.05 (m, 1 H), 1.01 (d, J = 6.6 Hz, 6 H). LC–HRMS: t_{R} = 1.45 min, $[\text{M} + \text{H}]^+ / z = 460.1906$, found = 460.1909.

(*S*)-3-(2-Ethyl-4-(5-(3-ethyl-5,5-dimethyl-4,5,6,7-tetrahydrobenzo[*c*]thiophen-1-yl)-1,2,4-oxadiazol-3-yl)-6-methylphenoxy)propane-1,2-diol (104). To a solution of 3-ethyl-5,5-dimethyl-4,5,6,7-tetrahydrobenzo[*c*]thiophene-1-carboxylic acid 10 (200 mg, 0.839 mmol) in DMF (5 mL) DIPEA (217 mg, 1.68 mmol) followed by TBTU (296 mg, 0.923 mmol) is added. The mixture is stirred at room temperature for 10 min before (*R*)-4-(2,2-dimethyl-1,3-dioxolan-4-ylmethoxy)-3-ethyl-*N*-hydroxy-5-methylbenzamidine (259 mg, 0.839 mmol) is added. Stirring is continued at room temperature for 1 h. The mixture is diluted with EA (100 mL), washed with water (50 mL), dried over MgSO_4 , filtered, and concentrated. The remaining residue is dissolved in dioxane (10 mL), and the mixture is stirred at 80 °C for 18 h, then at 100 °C for 48 h. The mixture is concentrated, and the crude product is purified on preparative TLC plates using heptane/EA 9:1 to give (*R*)-3-(4-((2,2-dimethyl-1,3-dioxolan-4-yl)methoxy)-3-ethyl-5-methylphenyl)-5-(3-ethyl-5,5-dimethyl-4,5,6,7-tetrahydrobenzo[*c*]thiophen-1-yl)-1,2,4-oxadiazole (217 mg, 51%) as a pale beige resin. LC–MS: t_{R} = 1.25 min, $[\text{M} + 1]^+ = 511.27$. This material is dissolved in 4 M HCl in dioxane (10 mL), and the mixture is stirred at room temperature for 18 h. The solvent is removed in vacuo and the crude product is purified by preparative HPLC to give the title compound 104 (160 mg, 80%). LC–MS: t_{R} = 1.10 min, $[\text{M} + 1]^+ = 471.28$. ^1H NMR (CDCl_3): δ 7.86 (s, 1 H), 7.85 (s, 1 H), 4.13–4.20 (m, 1 H), 3.82–3.99 (m, 4 H), 3.17 (t, J = 6.7 Hz, 2 H), 2.80 (q, J = 7.5 Hz, 2 H), 2.76 (q, J = 7.8 Hz, 2 H), 2.40 (s, 3 H), 2.38 (s, 2 H), 2.10 (s br, 1 H), 1.67 (t, J = 6.7 Hz, 2 H), 1.34 (t, J = 7.8 Hz, 3 H), 1.32 (t, J = 7.0 Hz, 3 H), 1.05 (s, 6 H). ^{13}C NMR (CDCl_3): δ 172.2, 168.1, 157.0, 147.7, 144.6, 137.5, 135.7, 131.5, 128.4, 126.7, 123.2, 115.2, 73.9, 71.0, 63.8, 38.5, 35.5, 29.6, 27.9, 24.3, 22.9, 21.6, 16.4, 14.9. LC–HRMS: t_{R} = 1.80 min, $[\text{M} + \text{H}]^+ / z = 471.2318$, found = 471.2315.

3-(2-Ethyl-4-(5-(3-ethyl-5,5-dimethyl-4,5,6,7-tetrahydrobenzo[*c*]thiophen-1-yl)-1,2,4-oxadiazol-3-yl)-6-methylphenyl)propanoic Acid (105). To a solution of 3-ethyl-5,5-dimethyl-4,5,6,7-tetrahydrobenzo[*c*]thiophene-1-carboxylic acid 10 (2.00 g, 8.39 mmol) in DMF (20 mL) DIPEA (3.25 g, 25.2 mmol) followed by TBTU (2.83 g, 8.81 mmol) is added. The mixture is stirred at room temperature for 5 min before 3-[2-ethyl-4-(*N*-hydroxycarbamimidoyl)-6-methylphenyl]propanoic acid (2.10 g, 8.39 mmol, Supporting Information) is added. Stirring is continued at room temperature for 2 h. Water (50 mL) and saturated aqueous NaHCO_3 solution (50 mL) are added, and the mixture is extracted twice with EA (2 \times 100 mL). The organic extracts are combined, dried over MgSO_4 , filtered, and concentrated. The residue is dissolved in dioxane (50 mL), and the mixture is stirred at 80 °C for 18 h. The solvent is evaporated and the crude product is purified by preparative HPLC to give the title compound 105 (2.85 g, 75%) as a white solid. LC–MS: t_{R} = 1.14 min, $[\text{M} + 1]^+ = 453.13$. ^1H NMR ($\text{DMSO}-d_6$): δ 12.28 (s br, 1 H), 7.69 (s, 1 H), 7.69 (s, 1 H), 3.07 (t, J = 6.6 Hz, 2 H), 2.90–2.96 (m, 2 H), 2.80 (q, J = 7.4 Hz, 2 H), 2.72 (q, J = 7.5 Hz, 2 H), 2.36–2.42 (m, 7 H), 1.62 (t, J = 6.6 Hz, 2 H), 1.25 (t, J = 7.5 Hz, 3 H), 1.22 (t, J = 7.5 Hz, 3 H), 0.99 (s, 6 H). ^{13}C NMR ($\text{DMSO}-d_6$): δ 174.2, 171.9, 168.1, 148.2, 144.9, 143.3, 141.2, 137.7, 136.3, 127.0, 125.3, 124.4, 114.6, 38.2, 35.1,

34.0, 29.7, 28.0, 25.7, 24.6, 24.3, 21.4, 19.9, 16.1, 15.2. LC–HRMS: t_{R} = 1.85 min, $[\text{M} + \text{H}]^+ / z = 453.2212$, found = 453.2209.

3-((2-(2-Ethyl-4-(5-(3-ethyl-5,5-dimethyl-4,5,6,7-tetrahydrobenzo[*c*]thiophen-1-yl)-1,2,4-oxadiazol-3-yl)-6-methylphenoxy)ethyl)amino)propanoic Acid (106). (a) To a solution of 2-ethyl-4-(5-(3-ethyl-5,5-dimethyl-4,5,6,7-tetrahydrobenzo[*c*]thiophen-1-yl)-1,2,4-oxadiazol-3-yl)-6-methylphenol (1.60 g, 4.03 mmol) in isopropanol (100 mL) and 3 M aqueous NaOH (40 mL) 2-bromoethanol (2.02 g, 16.1 mmol) is added, and the mixture is stirred at 65 °C for 18 h. Another portion of 2-bromoethanol (2.02 g, 16.1 mmol) is added, and stirring is continued at 65 °C for 48 h. The mixture is diluted with EA (250 mL) and washed with water (100 mL). The organic extract is dried over MgSO_4 , filtered, and concentrated. The crude product is purified by CC on silica gel, eluting with heptane/EA to give 2-(2-ethyl-4-(5-(3-ethyl-5,5-dimethyl-4,5,6,7-tetrahydrobenzo[*c*]thiophen-1-yl)-1,2,4-oxadiazol-3-yl)-6-methylphenoxy)ethanol (1.15 g, 65%) as a beige oil. LC–MS: t_{R} = 1.15 min, $[\text{M} + 1]^+ = 440.94$.

(b) To a solution of 2-(2-ethyl-4-(5-(3-ethyl-5,5-dimethyl-4,5,6,7-tetrahydrobenzo[*c*]thiophen-1-yl)-1,2,4-oxadiazol-3-yl)-6-methylphenoxy)ethanol (1.10 g, 2.50 mmol) in DCM triethylamine (354 mg, 3.50 mmol) is added. The mixture is cooled to 0 °C before methanesulfonyl chloride (343 mg, 3.00 mmol) is added. The mixture is stirred at 0 °C for 1 h, then at room temperature for 2 h before it is diluted with DCM (50 mL), washed with H_2O (50 mL), dried over MgSO_4 , filtered, and concentrated to give a crude mesylate intermediate (1.46 g, quantitative). LC–MS: t_{R} = 1.14 min, $[\text{M} + 1]^+ = 511.99$. This material is added to a solution of β -alanine methyl ester obtained by filtering a solution of the corresponding hydrochloride salt (471 mg, 3.37 mmol) in acetonitrile over Dowex Marathon ion-exchange resin (4 g, OH form). Triethylamine (49 mg, 0.482 mmol) is added, and the mixture is stirred at 80 °C for 96 h in a sealed vessel. The mixture is concentrated and the crude product is purified by preparative HPLC to give methyl 3-((2-(2-ethyl-4-(5-(3-ethyl-5,5-dimethyl-4,5,6,7-tetrahydrobenzo[*c*]thiophen-1-yl)-1,2,4-oxadiazol-3-yl)-6-methylphenoxy)ethyl)amino)propanoate which is dissolved in THF (5 mL), methanol (4 mL), and 3 M aqueous NaOH (1 mL). The mixture is stirred at room temperature for 8 h. The mixture is diluted with water acidified with aqueous HCl and extracted twice with DCM (2 \times 50 mL). The organic extracts are washed with brine, dried over MgSO_4 , filtered, concentrated, and dried to give the title compound 106 (115 mg, 47%) as a colorless resin. LC–MS: t_{R} = 0.92 min, $[\text{M} + 1]^+ = 512.05$. ^1H NMR (CDCl_3): δ 9.41 (s br, 2 H), 7.78 (s, 1 H), 7.74 (s, 1 H), 4.26 (t, J = 4.8 Hz, 2 H), 3.44–3.61 (m, 4 H), 3.08–3.20 (m, 4 H), 2.79 (q, J = 7.5 Hz, 2 H), 2.71 (q, J = 7.4 Hz, 2 H), 2.37–2.44 (m, 2 H), 2.36 (s, 2 H), 2.35 (s, 3 H), 1.65 (t, J = 6.8 Hz, 2 H), 1.32 (t, J = 7.5 Hz, 3 H), 1.29 (t, J = 8.0 Hz, 3 H), 1.04 (s, 6 H). ^1H NMR ($\text{DMSO}-d_6$): δ 7.76 (s, 2 H), 4.09 (t, J = 4.5 Hz, 2 H), 3.27 (t, J = 7.0 Hz, 2 H), 3.06 (t, J = 6.5 Hz, 2 H), 2.70–2.84 (m, 6 H), 2.38 (s, 5 H), 1.61 (t, J = 6.5 Hz, 2 H), 1.25 (t, J = 7.5 Hz, 3 H), 1.24 (t, J = 7.5 Hz, 3 H), 0.99 (s, 6 H). ^{13}C NMR ($\text{DMSO}-d_6$): δ 172.4, 172.0, 167.8, 157.3, 148.3, 145.1, 138.1, 136.4, 132.4, 128.3, 126.4, 122.9, 114.5, 68.3, 47.4, 43.6, 38.2, 35.1, 30.9, 29.7, 28.0, 24.3, 22.6, 21.4, 16.7, 15.3, 15.2. LC–HRMS: t_{R} = 1.35 min, $[\text{M} + \text{H}]^+ / z = 512.2583$, found = 512.2584.

■ ASSOCIATED CONTENT

Supporting Information

Experimental details on the synthesis and characterization of all target compounds and intermediates not described in the main text. This material is available free of charge via the Internet at <http://pubs.acs.org>.

■ AUTHOR INFORMATION

Corresponding Author

*Phone: +41 61 565 65 65. Fax: +41 61 565 65 00. E-mail: martin.bolli@actelion.com.

Notes

The authors declare no competing financial interest.

ACKNOWLEDGMENTS

The authors gratefully acknowledge their colleagues Stefan Abele, Céline Bortolamiol, Maxime Boucher, Stéphane Delahaye, Patrick Dörrwächter, Fabienne Drouet, Alexandre Flock, Julien Grimont, Hakim Hadana, Julie Hoerner, Benedikt Hofstetter, Heidemarie Kletzl, François LeGoff, Claire Maciejasz, Céline Mangold, Katalin Menyhart, Matthias Merrettig, Christine Metzger, Michel Rauser, Gunther Schmidt, Christine Seeger, Jürgen Seifert, Virginie Sippel, Mireille Tena Stern, Marco Tschanz, Gaby von Aesch, Daniel Wanner, Aude Weigel, and Rolf Wüst for the excellent work done and Martine Clozel and Thomas Weller for support.

ABBREVIATIONS USED

AcOH, acetic acid; BuLi, butyllithium; CC, column chromatography; DCM, dichloromethane; DEAD, diethyl azodicarbonylate; DMF, dimethylformamide; EA, ethyl acetate; EDC, 1-ethyl-3-(3-dimethylaminopropyl)carbodiimide; HOBt, *N*-hydroxybenzotriazole; HTS, high-throughput screening; HV, high vacuum; LC, lymphocyte count; LDA, lithium diisopropylamide; PK, pharmacokinetics; PD, pharmacodynamics; SAR, structure–activity relationship; TBTU, *O*-(benzotriazol-1-yl)-*N,N,N',N'*-tetramethyluronium tetrafluoroborate; THF, tetrahydrofuran; S1P, sphingosine 1-phosphate

REFERENCES

- (1) Liu, F.; Verin, A. D.; Wang, P.; Day, R.; Wersto, R. P.; Chrest, F. J.; English, D. K.; Garcia, J. G. N. Differential regulation of sphingosine-1-phosphate- and VEGF-induced endothelial cell chemotaxis. *Am. J. Respir. Cell Mol. Biol.* **2001**, *24*, 711–719.
- (2) Maceyka, M.; Payne, S. G.; Milstien, S.; Spiegel, S. Sphingosine kinase, sphingosine-1-phosphate, and apoptosis. *Biochim. Biophys. Acta* **2002**, *1585*, 193–201.
- (3) Graeler, M.; Goetzl, E. J. Activation-regulated expression and chemotactic function of sphingosine 1-phosphate receptors in mouse splenic T cells. *FASEB J.* **2002**, *16*, 1874–1878.
- (4) Dorsam, G.; Graeler, M. H.; Seroogy, C.; Kong, Y.; Voice, J. K.; Goetzl, E. J. Transduction of multiple effects of sphingosine 1-phosphate (S1P) on T cell functions by the S1P₁ G protein-coupled receptor. *J. Immunol.* **2003**, *171*, 3500–3507.
- (5) Baumruker, T.; Billich, A. Sphingolipids in cell signalling: their function as receptor ligands, second messengers, and raft constituents. *Curr. Immunol. Rev.* **2006**, *2*, 101–118.
- (6) Kihara, A.; Mitsutake, S.; Mizutani, Y.; Igarashi, Y. Metabolism and biological functions of two phosphorylated sphingolipids, sphingosine 1-phosphate and ceramide 1-phosphate. *Prog. Lipid Res.* **2007**, *46*, 126–144.
- (7) Brinkmann, V. Sphingosine 1-phosphate receptors in health and disease: mechanistic insights from gene deletion studies and reverse pharmacology. *Pharmacol. Ther.* **2007**, *115*, 84–105.
- (8) Hisano, Y.; Nishi, T.; Kawahara, A. The functional roles of S1P in immunity. *J. Biochem.* **2012**, *152*, 305–311.
- (9) Chun, J.; Goetzl, E. J.; Hla, T.; Igarashi, Y.; Lynch, K. R.; Moolenaar, W.; Pyne, S.; Tigyi, G. International Union of Pharmacology. XXXIV. Lysophospholipid receptor nomenclature. *Pharmacol. Rev.* **2002**, *54*, 265–269.
- (10) Ishii, I.; Fukushima, N.; Ye, X.; Chun, J. Lysophospholipid receptors: signaling and biology. *Annu. Rev. Biochem.* **2004**, *73*, 321–354.
- (11) Rosen, H.; Goetzl, E. J. Sphingosine 1-phosphate and its receptors: an autocrine and paracrine network. *Nat. Rev. Immunol.* **2005**, *5*, 560–570.
- (12) Meyer-zu-Heringdorf, D.; Jakobs, K. H. Lysophospholipid receptors: signalling, pharmacology and regulation by lysophospholipid metabolism. *Biochim. Biophys. Acta* **2006**, *1768*, 923–940.
- (13) Gardell, S. E.; Dubi, A. E.; Chun, J. Emerging medicinal roles for lysophospholipid signaling. *Trends Mol. Med.* **2006**, *12*, 65–75.
- (14) Okada, T.; Kajimoto, T.; Jahangeer, S.; Nakamura, S. Sphingosine kinase/sphingosine 1-phosphate signalling in central nervous system. *Cell. Signalling* **2009**, *21*, 7–13.
- (15) Milstien, S.; Gude, D.; Spiegel, S. Sphingosine 1-phosphate in neural signalling and function. *Acta Paediatr., Suppl.* **2007**, *96*, 40–43.
- (16) Brinkmann, V.; Baumruker, T. Pulmonary and vascular pharmacology of sphingosine 1-phosphate. *Curr. Opin. Pharmacol.* **2006**, *6*, 244–250.
- (17) Uhlig, S.; Gulbins, E. Sphingolipids in the lungs. *Am. J. Respir. Crit. Care Med.* **2008**, *178*, 1100–1114.
- (18) Augé, N.; Nègre-Salvayre, A.; Salvayre, R.; Levade, T. Sphingomyelin metabolites in vascular cell signaling and atherogenesis. *Prog. Lipid Res.* **2000**, *39*, 207–229.
- (19) Alewijnse, A. E.; Peters, S. L. M.; Michel, M. C. Cardiovascular effects of sphingosine-1-phosphate and other sphingomyelin metabolites. *Br. J. Pharmacol.* **2004**, *143*, 666–684.
- (20) McVerry, B. J.; Garcia, J. G. N. In vitro and in vivo modulation of vascular barrier integrity by sphingosine 1-phosphate: mechanistic insights. *Cell. Signalling* **2005**, *17*, 131–139.
- (21) Yatomi, Y. Sphingosine 1-phosphate in vascular biology: possible therapeutic strategies to control vascular disease. *Pharm. Des.* **2006**, *12*, 575–587.
- (22) Rosen, H.; Sanna, M. G.; Cahalan, S. M.; Gonzalez-Cabrera, P. J. Tipping the gatekeeper: S1P regulation of endothelial barrier function. *Trends Immunol.* **2007**, *28*, 102–107.
- (23) Michel, M. C.; Mulders, A. C. M.; Jongsma, M.; Alewijnse, A. E.; Peters, S. L. M. Vascular effects of sphingolipids. *Acta Paediatr., Suppl.* **2007**, *96*, 44–48.
- (24) Alewijnse, A. E.; Peters, S. L. M. Sphingolipid signalling in the cardiovascular system: good, bad or both? *Eur. J. Pharmacol.* **2008**, *585*, 292–302.
- (25) Okamoto, Y.; Wang, F.; Yoshioka, K.; Takuwa, N.; Takuwa, Y. Sphingosine-1-phosphate-specific G protein-coupled receptors as novel therapeutic targets for atherosclerosis. *Pharmaceuticals* **2011**, *4*, 117–137.
- (26) Lucke, S.; Levkau, B. Endothelial functions of sphingosine-1-phosphate. *Cell. Physiol. Biochem.* **2010**, *26*, 87–96.
- (27) Oskeritzian, C. A.; Milstien, S.; Spiegel, S. Sphingosine-1-phosphate in allergic responses, asthma and anaphylaxis. *Pharmacol. Ther.* **2007**, *115*, 390–399.
- (28) Rivera, A.; Proia, R. L.; Olivera, A. The alliance of sphingosine-1-phosphate and its receptors in immunity. *Nat. Rev. Immunol.* **2008**, *8*, 753–763.
- (29) Ishii, M.; Egen, J. G.; Klauschen, F.; Meier-Schellersheim, M.; Saeki, Y.; Vacher, J.; Proia, R. L.; Germain, R. N. Sphingosine-1-phosphate mobilizes osteoclast precursors and regulates bone homeostasis. *Nature* **2009**, *458*, 524–528.
- (30) Huwiler, A.; Pfeilschifter, J. New players on the center stage: sphingosine 1-phosphate and its receptors as drug targets. *Biochem. Pharmacol.* **2008**, *75*, 1893–1900.
- (31) Pyne, N. J.; Tonelli, F.; Lim, K. G.; Long, J. S.; Edwards, J.; Pyne, S. Sphingosine 1-phosphate signalling in cancer. *Biochem. Soc. Trans.* **2012**, *40*, 94–100.
- (32) Maceyka, M.; Harikumar, K. B.; Milstien, S.; Spiegel, S. Sphingosine-1-phosphate signaling and its role in disease. *Trends Cell Biol.* **2012**, *22*, 50–60.
- (33) Adachi, K.; Kohara, T.; Nakao, N.; Arita, M.; Chiba, K.; Mishina, T.; Sasaki, S.; Fujita, T. Design, synthesis, and structure–activity relationships of 2-substituted-2-amino-1,3-propanediols: discovery of a novel immunosuppressant, FTY720. *Bioorg. Med. Chem. Lett.* **1995**, *5*, 853–856.
- (34) Chiba, K.; Yanagawa, Y.; Masubuchi, Y.; Kataoka, H.; Kawaguchi, T.; Ohtsuki, M.; Hoshino, Y. FTY720, a novel immunosuppressant, induces sequestration of circulating mature

lymphocytes by acceleration of lymphocyte homing in rats. I. FTY720 selectively decreases the number of circulating mature lymphocytes by acceleration of lymphocyte homing. *J. Immunol.* **1998**, *160*, 5037–5044.

(35) Pinschewer, D. D.; Ochsenbein, A. F.; Odermatt, B.; Brinkmann, V.; Hengartner, H.; Zinkernagel, R. M. FTY720 immunosuppression impairs effector T cell peripheral homing without affecting induction, expansion, and memory. *J. Immunol.* **2000**, *164*, 5761–5770.

(36) Brinkmann, V.; Chen, S.; Feng, L.; Pinschewer, D.; Nikolova, Z.; Hof, R. FTY720 alters lymphocyte homing and protects allografts without inducing general immunosuppression. *Transplant. Proc.* **2001**, *33*, 530–531.

(37) Brinkmann, V.; Davis, M. D.; Heise, C. E.; Albert, R.; Cottens, S.; Hof, R.; Bruns, C.; Prieschl, E.; Baumruker, T.; Hiestand, P.; Foster, C. A.; Zollinger, M.; Lynch, K. R. The immune modulator FTY720 targets sphingosine 1-phosphate receptors. *J. Biol. Chem.* **2002**, *277*, 21453–21457.

(38) Billich, A.; Bornancin, F.; Dévay, P.; Mechtcheriakova, D.; Urtz, N.; Baumruker, T. Phosphorylation of the immunomodulatory drug FTY720 by sphingosine kinases. *J. Biol. Chem.* **2003**, *278*, 47408–47415.

(39) Mandala, S.; Hajdu, R.; Bergstrom, J.; Quackenbush, E.; Xie, J.; Milligan, J.; Thornton, R.; Shei, G.-J.; Card, D.; Keohane, C. A.; Rosenbach, M.; Hale, J.; Lynch, C. L.; Rupprecht, K.; Parsons, W.; Rosen, H. Alteration of lymphocyte trafficking by sphingosine-1-phosphate receptor agonists. *Science* **2002**, *296*, 346–349.

(40) Sobel, K.; Menyhart, K.; Killer, N.; Renault, B.; Bauer, Y.; Studer, R.; Steiner, B.; Bolli, M. H.; Nayler, O.; Gatfield, J. Sphingosine-1-phosphate (S1P) receptor agonists mediate pro-fibrotic responses in normal human lung fibroblasts via S1P₂ and S1P₃ receptors and Smad-independent signaling. *J. Biol. Chem.* **2013**, *288*, 14839–14851.

(41) Hla, T.; Venkataraman, K.; Michaud, J. The vascular S1P gradient: cellular sources and biological significance. *Biochim. Biophys. Acta* **2008**, *1781*, 477–482.

(42) Schwab, S. R.; Cyster, J. G. Finding a way out: lymphocyte egress from lymphoid organs. *Nat. Immunol.* **2007**, *8*, 1295–1301.

(43) Pappu, R.; Schwab, S. R.; Cornelissen, L.; Pereira, J. P.; Regard, J. B.; Xu, Y.; Camerer, E.; Zheng, Y.-W.; Huang, Y.; Cyster, J. G.; Coughlin, S. R. Promotion of lymphocyte egress into blood and lymph by distinct sources of sphingosine-1-phosphate. *Science* **2007**, *316*, 295–298.

(44) Fujii, Y.; Ohtake, H.; Ono, N.; Hara, T.; Sakurai, T.; Takahashi, S.; Takayama, T.; Fukasawa, Y.; Shiozawa, F.; Tsukahara, N.; Hirayama, T.; Igarashi, Y.; Goitsuka, R. Lymphopenia induced by a novel selective S1P₁ antagonist structurally unrelated to S1P. *Biochim. Biophys. Acta* **2012**, *1821*, 600–606.

(45) Quancard, J.; Bollbuck, B.; Janser, P.; Angst, D.; Berst, F.; Buehlmaier, P.; Streiff, M.; Beerli, C.; Brinkmann, V.; Guerini, D.; Smith, P. A.; Seabrook, T. J.; Traebert, M.; Seuwen, K.; Hersperger, R.; Bruns, C.; Bassilana, F.; Bigaud, M. A potent and selective S1P₁ antagonist with efficacy in experimental autoimmune encephalomyelitis. *Chem. Biol.* **2012**, *19*, 1142–1151.

(46) Allende, M. L.; Dreier, J. L.; Mandala, S.; Proia, R. L. Expression of the sphingosine 1-phosphate receptor, S1P₁, on T-cells controls thymic emigration. *J. Biol. Chem.* **2004**, *279*, 15396–15401.

(47) Matloubian, M.; Lo, C. G.; Cinamon, G.; Lesneski, M. J.; Xu, Y.; Brinkmann, V.; Allende, M. L.; Proia, R. L.; Cyster, J. G. Lymphocyte egress from thymus and peripheral lymphoid organs is dependent on S1P receptor 1. *Nature* **2004**, *427*, 355–360.

(48) Hale, J. J.; Neway, W.; Mills, S. G.; Hajdu, R.; Keohane, C. A.; Rosenbach, M.; Milligan, J.; Shei, G.-J.; Chrebet, G.; Bergstrom, J.; Card, D.; Koo, G. C.; Koprak, S. L.; Jackson, J. J.; Rosen, H.; Mandala, S. Potent S1P receptor agonists replicate the pharmacologic actions of the novel immune modulator FTY720. *Bioorg. Med. Chem. Lett.* **2004**, *14*, 3351–3355.

(49) Jo, E.; Sanna, M. G.; Gonzalez-Cabrera, P. J.; Thangada, S.; Tigyi, G.; Osborne, D. A.; Hla, T.; Parrill, A. L.; Rosen, H. S1P₁-

selective in vivo-active agonists from high-throughput screening: off-the-shelf chemical probes of receptor interactions, signaling, and fate. *Chem. Biol.* **2005**, *12*, 703–715.

(50) Wei, S. H.; Rosen, H.; Matheu, M. P.; Sanna, M. G.; Wang, S.-K.; Jo, E.; Wong, C.-H.; Parker, I.; Cahalan, M. D. Sphingosine 1-phosphate type 1 receptor agonism inhibits transendothelial migration of medullary T cells to lymphatic sinuses. *Nat. Immunol.* **2005**, *6*, 1228–1235.

(51) Hale, J. J.; Doherty, G.; Toth, L.; Mills, S. G.; Hajdu, R.; Keohane, C. A.; Rosenbach, M.; Milligan, J.; Shei, G.-J.; Chrebet, G.; Bergstrom, J.; Card, D.; Forrest, M.; Sun, S.-Y.; West, S.; Xie, H.; Nomura, N.; Rosen, H.; Mandala, S. Selecting against S1P₃ enhances the acute cardiovascular tolerability of 3-(N-benzyl)-aminopropylphosphonic acid S1P receptor agonists. *Bioorg. Med. Chem. Lett.* **2004**, *14*, 3501–3505.

(52) Sanna, M. G.; Liao, J.; Jo, E.; Alfonso, C.; Ahn, M.-Y.; Peterson, M. S.; Webb, B.; Lefebvre, S.; Chun, J.; Gray, N.; Rosen, H. Sphingosine 1-phosphate (S1P) receptor subtypes S1P₁ and S1P₃, respectively, regulate lymphocyte recirculation and heart rate. *J. Biol. Chem.* **2004**, *279*, 13839–13848.

(53) Forrest, M.; Sun, S.-Y.; Hajdu, R.; Bergstrom, J.; Card, D.; Doherty, G.; Hale, J.; Keohane, C.; Meyers, C.; Milligan, J.; Mills, S.; Nomura, N.; Rosen, H.; Rosenbach, M.; Shei, G.-J.; Singer, I. I.; Tian, M.; West, S.; White, V.; Xie, J.; Proia, R. L.; Mandala, S. Immune cell regulation and cardiovascular effects of sphingosine 1-phosphate receptor agonists in rodents are mediated via distinct receptor subtypes. *J. Pharmacol. Exp. Ther.* **2004**, *309*, 758–768.

(54) Salomone, S.; Potts, E. M.; Tyndall, S.; Ip, P. C.; Chun, J.; Brinkmann, V.; Waeber, C. Analysis of sphingosine 1-phosphate receptors involved in constriction of isolated cerebral arteries with receptor null mice and pharmacological tools. *Br. J. Pharmacol.* **2008**, *153*, 140–147.

(55) Murakami, A.; Taksugi, H.; Ohnuma, S.; Koide, Y.; Sakurai, A.; Takeda, S.; Hasegawa, T.; Sasamori, J.; Konno, T.; Hayashi, K.; Watanabe, Y.; Mori, K.; Sato, Y.; Takahashi, A.; Mochizuki, N.; Takakura, N. Sphingosine 1-phosphate (S1P) regulates vascular contraction via S1P₃ receptor: investigation based on a new S1P₃ receptor antagonist. *Mol. Pharmacol.* **2010**, *77*, 704–713.

(56) Hamada, M.; Nakamura, M.; Kiuchi, M.; Marukawa, K.; Tomatsu, A.; Shimano, K.; Sato, N.; Sugahara, K.; Asayama, M.; Takagi, K.; Adachi, K. Removal of sphingosine 1-phosphate receptor-3 (S1P₃) agonism is essential, but inadequate to obtain immunomodulating 2-aminopropane-1,3-diol S1P₁ agonists with reduced effect on heart rate. *J. Med. Chem.* **2010**, *53*, 3154–3168.

(57) Fryer, R. M.; Muthukumarana, A.; Harrison, P. C.; Nodop Mazurek, S.; Chen, R. R.; Harrington, K. E.; Dinallo, R. M.; Horan, J. C.; Patnaude, L.; Modis, L. K.; Reinhart, G. A. The clinically-tested S1P receptor agonists, FTY720 and BAF312, demonstrate subtype-specific bradycardia (S1P(1)) and hypertension (S1P(3)) in rat. *PLoS One* **2012**, *7*, e25985.

(58) Brossard, P.; Hofmann, S.; Cavallaro, M.; Halabi, A.; Dingemans, J. Entry-into-Humans Study with ACT-128800, a Selective S1P₁ Receptor Agonist: Tolerability, Safety, Pharmacokinetics, and Pharmacodynamics. Presented at ASCPT 2009, Annual Meeting of the American Society for Clinical Pharmacology and Therapeutics, Washington DC, USA, March 18–21, 2009; PII-87; *Clin. Pharmacol. Ther.* **2009**, S63–S64.

(59) Gergely, P.; Wallström, E.; Nuesslein-Hildesheim, B.; Bruns, C.; Zéciri, F. J.; Cooke, N. G.; Traebert, M.; Tuntland, T.; Rosenberg, M.; Saltzman, M. Phase I Study with the Selective S1P₁/S1P₅ Receptor Modulator BAF312 Indicates That S1P₁ Rather Than S1P₃ Mediates Transient Heart Rate Reduction in Humans. Presented at the 25th Congress of the European Committee for Treatment and Research in Multiple Sclerosis (ECTRIMS), Düsseldorf, Germany, 2009; P437.

(60) Wallström, E.; Gergely, P.; Nuesslein-Hildesheim, B.; Zéciri, F. J.; Cooke, N. G.; Bruns, C.; Luttringer, O.; Sing, T.; Groenewegen, A.; Rosenberg, M.; Saltzman, M. BAF312, a Selective S1P₁/S1P₅ Receptor Modulator, Effectively Reduces Absolute Lymphocyte Counts in Human Volunteers and Demonstrates the Relevance of

S1P1 in Mediating a Transient Heart Rate Reduction. Presented at the 62nd Annual Meeting of the American Academy of Neurology, Toronto, Ontario, Canada, 2010; PO5.052.

(61) Gergely, P.; Nuesslein-Hildesheim, B.; Guerini, D.; Brinkmann, V.; Traebert, M.; Bruns, C.; Pan, S.; Gray, N. S.; Hinterding, K.; Cooke, N. G.; Groenewegen, A.; Vitaliti, A.; Sing, T.; Luttringer, O.; Yang, J.; Gardin, A.; Wang, N.; Crumb, W. J. J.; Saltzman, M.; Rosenberg, M.; Wallström, E. The selective S1P receptor modulator BAF312 redirects lymphocyte distribution and has species-specific effects on heart rate: translation from preclinical to clinical studies. *Br. J. Pharmacol.* **2012**, *167*, 1035–1047.

(62) Brinkmann, V.; Billich, A.; Baumruker, T.; Heining, P.; Schmouder, R.; Francis, G.; Aradhye, S.; Burtin, P. Fingolimod (FTY720): discovery and development of an oral drug to treat multiple sclerosis. *Nat. Rev. Drug Discovery* **2010**, *9*, 883–897.

(63) Aktas, O.; Küry, P.; Kieseier, B.; Hartung, H.-P. Fingolimod is a potential novel therapy for multiple sclerosis. *Nat. Rev. Neurol.* **2010**, *6*, 373–382.

(64) Ingwersen, J.; Aktas, O.; Kuery, P.; Kieseier, B.; Boyko, A.; Hartung, H.-P. Fingolimod in multiple sclerosis: mechanisms of action and clinical efficacy. *Clin. Immunol.* **2012**, *142*, 15–24.

(65) Bolli, M. H.; Abele, S.; Binkert, C.; Bravo, R.; Buchmann, S.; Bur, D.; Gatfield, J.; Hess, P.; Kohl, C.; Mangold, C.; Mathys, B.; Menyhart, K.; Müller, C.; Nayler, O.; Scherz, M.; Schmidt, G.; Sippel, V.; Steiner, B.; Strasser, D.; Treiber, A.; Weller, T. 2-Imino-thiazolidin-4-one derivatives as potent, orally active S1P1 receptor agonists. *J. Med. Chem.* **2010**, *53*, 4198–4211.

(66) ClinicalTrials.gov. Ponesimod in Patients with Relapsing-Remitting Multiple Sclerosis: Extension Study. <http://clinicaltrials.gov/show/NCT01093326> (accessed Aug 2012).

(67) ClinicalTrials.gov. ACT-128800 in Relapsing-Remitting Multiple Sclerosis. <http://clinicaltrials.gov/show/NCT01006265> (accessed Aug 2012).

(68) ClinicalTrials.gov. ACT-128800 in Patients with Moderate to Severe Chronic Plaque Psoriasis. <http://clinicaltrials.gov/show/NCT01208090> (accessed Aug 2012).

(69) Pan, S.; Gray, N.; Gao, W.; Mi, Y.; Fan, Y.; Wang, X.; Tuntland, T.; Che, J.; Lefebvre, S.; Chen, Y.; Chu, A.; Hinterding, K.; Gardin, A.; End, P.; Heining, P.; Bruns, C.; Cooke, N. G.; Nuesslein-Hildesheim, B. Discovery of BAF312 (siponimod), a potent and selective S1P receptor modulator. *ACS Med. Chem. Lett.* **2013**, *4*, 333–337.

(70) ClinicalTrials.gov. Long-Term Safety, Tolerability and Efficacy with BAF312 Given Orally in Patients with Relapsing-Remitting Multiple Sclerosis. <http://clinicaltrials.gov/show/NCT01185821> (accessed Aug 2012).

(71) ClinicalTrials.gov. Safety, Tolerability, Efficacy and Optimal Dose Finding Study of BAF312 in Patients with Relapsing-Remitting Multiple Sclerosis. <http://clinicaltrials.gov/show/NCT00879658> (accessed Aug 2012).

(72) ClinicalTrials.gov. A Study of the Safety and Efficacy of ONO-4641 in Patients with Relapsing-Remitting Multiple Sclerosis (DreaMS). <http://clinicaltrials.gov/show/NCT01081782> (accessed Aug 2012).

(73) Nishi, T.; Miyazaki, S.; Takemoto, T.; Suzuki, K.; Iio, Y.; Nakajima, K.; Ohnuki, T.; Kawase, Y.; Nara, F.; Inaba, S.; Izumi, T.; Yuita, H.; Oshima, K.; Doi, H.; Inoue, R.; Tomisato, W.; Kagari, T.; Shimozato, T. Discovery of CS-0777: a potent, selective, and orally active S1P₁ agonist. *ACS Med. Chem. Lett.* **2011**, *2*, 368–372.

(74) Moberly, J. B.; Ford, D. M.; Zahir, H.; Chen, S.; Mochizuki, T.; Truitt, K. E.; Vollmer, T. L. Pharmacological effects of CS-0777, a selective sphingosine 1-phosphate receptor-1 modulator: results from a 12-week, open-label pilot study in multiple sclerosis patients. *J. Neuroimmunol.* **2012**, *246*, 100–107.

(75) Shimizu, H.; Takahashi, M.; Kaneko, T.; Murakami, T.; Hakamata, Y.; Kudou, S.; Kishi, T.; Fukuchi, K.; Iwanami, S.; Kuriyama, K.; Yasue, T.; Enosawa, S.; Matsumoto, K.; Takeyoshi, I.; Morishita, Y.; Kobayashi, E. KRP-203, a novel synthetic immunosuppressant, prolongs graft survival and attenuates chronic rejection in rat skin and heart allografts. *Circulation* **2005**, *111*, 222–229.

(76) ClinicalTrials.gov. Safety and Efficacy of KRP203 in Subacute Cutaneous Lupus Erythematosus. <http://clinicaltrials.gov/show/NCT01294774> (accessed July 2013).

(77) ClinicalTrials.gov. Efficacy & Safety in Moderately Active Refractory Ulcerative Colitis Patients. <http://clinicaltrials.gov/show/NCT01375179> (accessed July 2013).

(78) ClinicalTrials.gov. Efficacy and Safety Study of RPC1063 in Relapsing Multiple Sclerosis Patients. <http://clinicaltrials.gov/show/NCT01628393> (accessed July 2013).

(79) ClinicalTrials.gov. Dose Finding Study of MT-1303. <http://clinicaltrials.gov/show/NCT01742052> (accessed Jan 2013).

(80) Buzard, D. J.; Thatte, J.; Lerner, M.; Edwards, J.; Jones, R. M. Recent progress in the development of selective S1P₁ receptor agonists for the treatment of inflammatory and autoimmune disorders. *Expert Opin. Ther. Pat.* **2008**, *18*, 1141–1159.

(81) Bolli, M. H.; Lescop, C.; Nayler, O. Synthetic sphingosine 1-phosphate receptor modulators: opportunities and potential pitfalls. *Curr. Top. Med. Chem.* **2011**, *11*, 726–757.

(82) Dyckman, A. J. Recent advances in the discovery and development of sphingosine-1-phosphate-1 receptor agonists. *Annu. Rep. Med. Chem.* **2012**, *47*, 195–207.

(83) Roberts, E.; Guerrero, M.; Urbano, M.; Rosen, H. Sphingosine 1-phosphate receptor agonists: a patent review (2010–2012). *Expert Opin. Ther. Pat.* **2013**, *23*, 817–841.

(84) Bolli, M. H.; Müller, C.; Mathys, B.; Abele, S.; Birker, M.; Bravo, R.; Bur, D.; Hess, P.; Kohl, C.; Lehmann, D.; Nayler, O.; Rey, M.; Meyer, S.; Scherz, M.; Schmidt, G.; Steiner, B.; Treiber, A.; Velker, J.; Weller, T. Novel S1P₁ receptor agonists - Part 1: From pyrazoles to thiophenes. *J. Med. Chem.* **2013**, *56*, 9737–9755.

(85) Alberola, A.; Andres, J. M.; Gonzalez, A.; Pedrosa, R.; Pradanos, P. Regioselective synthesis of 2-functionalized thiophenes by condensation of α -mercapto compounds with β -amino enone derivatives. *Synth. Commun.* **1990**, *20*, 2537–2547.

(86) Kubiak, G. G.; Lythgoe, D. J.; Yu, Y. Regio-Specific Synthesis of 4-Bromo-3-methyl-5-propoxy-thiophene-2-carboxylic Acid. WO2008115912, Sep 25, 2008.

(87) Nahm, S.; Weinreb, S. M. *N*-Methoxy-*N*-methylamides as effective acylating agents. *Tetrahedron Lett.* **1981**, *22*, 3815–3818.

(88) Su, D.-B.; Duan, J.-X.; Chen, Q.-Y. Methyl chlorodifluoroacetate a convenient trifluoromethylating agent. *Tetrahedron Lett.* **1991**, *32*, 7689–7690.

(89) Bolli, M.; Lehmann, D.; Mathys, B.; Mueller, C.; Nayler, O.; Velker, J.; Weller, T. Novel Thiophene Derivatives. WO2006100635, Sep 28, 2006.

(90) Flough, M. A.; Crowell, T. A.; Farlow, D. S. Acid-catalyzed annelation of α -alkyl aldehydes and α,β -unsaturated ketones. A one-pot synthesis of 4,4-dimethyl-2-cyclohexen-1-one. *J. Org. Chem.* **1980**, *45*, 5399–5400.

(91) Wuesthoff, M. T.; Rickborn, B. The preparation of spiro[2.5]octan-6-one. Catalytic hydrogenation of a vinylcyclopropane. *J. Org. Chem.* **1968**, *33*, 1311–1312.

(92) Nicolaou, K. C.; Magolda, R. L.; Claremon, D. A. Carboxylic thromboxane A₂. *J. Am. Chem. Soc.* **1980**, *102*, 1404–1409.

(93) Arai, I.; Mori, A.; Yamamoto, H. An asymmetric Simmons–Smith reaction. *J. Am. Chem. Soc.* **1985**, *107*, 8254–8256.

(94) Mihovilovic, M. D.; Chen, G.; Wang, S.; Kyte, B.; Rochon, F.; Kayser, M. M.; Stewart, J. D. Asymmetric Bayer–Villiger oxidations of 4-mono- and 4,4-disubstituted cyclohexanones by whole cells of engineered *Escherichia coli*. *J. Org. Chem.* **2001**, *66*, 733–738.

(95) Natale, N. R.; Hutchins, R. O. An efficient, general synthesis of spiroalkanes and related derivatives. *Org. Prep. Proced. Int.* **1977**, *9*, 103–108.

(96) Knight, D. W.; Nott, A. P. Generation and synthetic utility of dianions derived from thiophenecarboxylic acids. *J. Chem. Soc., Perkin Trans. 1* **1983**, *1983*, 791–794.

(97) Gonzalez-Cabrera, P. J.; Cahalan, S. M.; Nguyen, N.; Sarkisyan, G.; Leaf, N. B.; Cameron, M. D.; Kago, T.; Rosen, H. S1P1 receptor modulation with cyclical recovery from lymphopenia ameliorates

mouse model of multiple sclerosis. *Mol. Pharmacol.* **2012**, *81*, 166–174.

(98) Meng, Q.; Zhao, B.; Xu, Q.; Xu, X.; Deng, G.; Li, C.; Luan, L.; Ren, F.; Wang, H.; Xu, H.; Xu, Y.; Zhang, H.; Xiang, J.-N.; Elliott, J. D.; Guo, T. B.; Zhao, Y.; Zhang, W.; Lu, H.; Lin, X. Indole-propionic acid derivatives as potent, S1P₃-sparing and EAE efficacious sphingosine-1-phosphate 1 (S1P₁) receptor agonists. *Bioorg. Med. Chem. Lett.* **2012**, *22*, 2794–2797.

(99) Rey, M.; Hess, P.; Clozel, M.; Delahaye, S.; Gatfield, J.; Nayler, O.; Steiner, B. Desensitization by progressive up-titration prevents first-dose effects on the heart: guinea pig study with ponesimod, a selective S1P1 receptor modulator. *PLoS One* **2013**, *8*, e74285.

(100) Wasan, K. M. The role of lymphatic transport in enhancing oral protein and peptide drug delivery. *Drug Dev. Ind. Pharm.* **2002**, *28*, 1047–1058.

(101) Yañez, J. A.; Wang, S. W. J.; Knemeyer, I. W.; Wirth, M. A.; Alton, K. B. Intestinal lymphatic transport for drug delivery. *Adv. Drug Delivery Rev.* **2011**, *63*, 923–942.

(102) Wagner, J.; von Matt, P.; Faller, B.; Cooke, N. G.; Albert, R.; Sedrani, R.; Wiegand, H.; Jean, C.; Beerli, C.; Weckebecker, G.; Evenou, J.-P.; Zenke, G.; Cottens, S. Structure–activity relationship and pharmacokinetic studies of sotrastaurin (AEB071), a promising novel medicine for prevention of graft rejection and treatment of psoriasis. *J. Med. Chem.* **2011**, *54*, 6028–6039.

(103) Grimont, J.; Le Goff, F.; Bourquin, G.; Silva, J. Quality Assessment and Concentration Determination of Actelion's Compound Solutions by Automated LCMS and Quantitative NMR. Presented at MipTec: The Leading European Event for Drug Discovery, Basel, Switzerland, Sep 20–24, 2010.

(104) Seglen, P. O.; Fosså, J. Attachment of rat hepatocytes in vitro to substrata of serum protein collagen, or concanavalin A. *Exp. Cell Res.* **1978**, *116*, 199–206.

(105) Obach, R. S. The prediction of human clearance from hepatic microsomal metabolism data. *Curr. Opin. Drug Discovery Dev.* **2001**, *4*, 36–44.

(106) Armarego, W. L. F.; Chai, C. L. L. *Purification of Laboratory Chemicals*, 6th ed.; Elsevier: Amsterdam, 2009.

(107) Buxbaum, E. *Biophysical Chemistry of Proteins: An Introduction to Laboratory Methods*; Springer: New York, 2011.